COMMERCIAL AEEW - M 312

The Sixth Core in DIMPLE at A.E.E. Winfrith

Experimental Results

by

A. G. Collins
W. A. V. Brown
W. H. Taylor
G. M. Wells

including work by

M. Singleton
Mrs. J. M. Symes

Abstract

The results obtained during experiments on the sixth SGHW core in DIMPLE are presented in this report in the form of raw data. No attempt to apply theoretical corrections to allow comparison with theory has been made, since this will be included in a more general report covering the whole series of SGHW experiments carried out at Winfrith.

The report is intended to provide a record of all important results obtained on this core. For the sake of brevity it refers frequently to the reports on the first five cores (1), (2), (3), and is only a complete record when used in conjunction with these references. Less essential details are recorded in the original experimental log books.

A.E.E.,
Winfrith.

March 1964.

W.6263

CONTENTS

FIGURES (Continued)

1. Introduction

This report describes the experiments carried out on the sixth of a series of cores built in the zero energy reactor DIMPLE in support of the general investigation of the reactor physics of Steam Generating Heavy Water (SGHW) reactors which has been undertaken by the Water Reactor Physics Division at A.E.E. Winfrith. The experiments in the earlier cores are reported in references (1) to (3) inclusive, and those in later cores will be described in further reports of this series. A companion series of papers covering the DIMPLE experiments and the work undertaken in sub-critical assemblies will be issued to compare the experimental data with theoretical predictions based on the methods of calculation in current use at Winfrith.

Reference (1), being the first of the series, described most of the experimental techniques in some detail, and reference (3) described the techniques for two additional experiments. For the sake of brevity, no such descriptions have been repeated in this report.

The previous core [(3)] consisted of a central region of 24 channels with mixed enrichment fuel cooled by light water, surrounded by 16 channels of fuel (identical to the second core [(2)]) acting as a driver region, the whole core then being surrounded by a D_2O reflector. In this present core the only difference was in the coolant used in the central 24 channels, which was changed to 70.3 ± 0.1% D_2O and 29.7% H_2O by weight. This mixture has a value of $\xi\Sigma_s$ which corresponds quite closely to that of light water with a density in the region of 0.4 gm cm^{-3}, which is typical of the average density within a boiling channel of an SGHW power reactor. The central region under study was "driven" by an outer region of sixteen pressure tubes of the identical core design reported in the second report [(2)] of this series.

2. Description of DIMPLE as constructed for this experiment

Except for the amount and type of fuel, and the number of fuel channels, the reactor was precisely as described in reference (1).

The core in the present report differs from the third core [(3)] only in the coolant used in the centre twenty four channels.

Figure 1 gives a plan view of the reactor tank and Figure 2 shows details of an inner zone lattice cell, with axial distances relative to search tubes and safety rods. Figure 3 is a detailed sketch of the inner zone fuel element and Figure 4 is a section through the reactor (a) in detail and (b) simplified for purposes of calculation [see Appendix I].

3. Approach to critical

At the completion of work on the third core, the fuel from the central twenty four channels was unloaded and dried, the pressure tubes were dried, and the fuel was then replaced. The H_2O/D_2O mixture (approx. 9.9. Kgm per tube) was then added, tube by tube, commencing at the centre. Throughout these operations a 10 curie Po-Be source was installed near the centre of the tank bottom and the flux as indicated by the three installed BF_3 chambers was recorded at frequent intervals. There was little change at any time, as expected from experience with earlier cores, indicating that the multiplication of such cores in the absence of the main D_2O moderator was very small.

Taking advantage of the conclusions reached in the earlier experiments (see in particular reference (1)) experimental BF_3 chambers were situated outside the fuelled part of the core and as remote from the source as was possible; the standard [1] approach to critical procedure was followed. The critical height was measured to be 151.00 cm (from the tank bottom) with all instruments removed from the core.

4. Reactivity measurements

All reactivity measurements have been normalised to a scale calibrated by the steady diverging period of the super-critical reactor. This was calculated by the method of reference (1) Appendix II.

In principle the reactivity-doubling time relation for a multi-zone reactor may be calculated using a statistical weighting procedure. Since, however, the difference between the scales used in the first (air-cooled) and second (water-cooled) cores was everywhere less that 1% of the reactivity, and between the first and seventh (air-cooled 1.9 Co) cores was everywhere less than 3% of the reactivity, [2] the scale for the second core was adopted for the fifth and sixth cores. Any error incurred is likely to be less than $\pm$ 1.5% of the reactivity measured. The table of values relating doubling time to reactivity is given in reference (2).

The method for measuring the steady doubling time of the divergent reactor was as described in reference (1). The sub-critical multiplication method adopted for measuring reactivities was also as described in reference (1), with the method for normalising to the supercritical scale as described in reference (2).

Table I below summarises the reactivity changes measured by super-critical methods. The reactivity worth of items has been computed by the change of critical height multiplied by the arithmetic mean of the values of $\partial\rho/\partial h$ at the two extreme moderator heights. All the values of $\partial\rho/\partial h$ are plotted against the arithmetic mean of the critical and divergent heights in Figure 5, and the values of $\partial\rho/\partial h$ shown in Table I are read off the dotted curve. Note that this curve has been drawn through the control rod results only, and, as in the earlier cores, the values of $\partial\rho/\partial h$ measured with fuel clusters missing lie well above it.

The errors quoted on the critical heights were deduced from repeated measurements on the HERRIOT MK I depth probe and represent the spread of observations under steady conditions. The error on the absolute height was of order 0.05 cm. The errors quoted on the reactivity changes are almost entirely due to the random error on the measurement of doubling time, which is about 1%. An additional systematic error of at least $\pm$ 5%, due to uncertainties in delayed neutron data and knowledge of β_{eff} (including photo-neutrons) must be taken into account before comparing these results with theory.

From Figure 5, the value of $\partial\rho/\partial h$ at the clean critical height was deduced to be $0.115 \pm .001\%\ cm^{-1}$. The value of $\partial\rho/\partial h$ measured with a near central pressure tube removed was about 5 ± 1.5 percent higher than that measured at approximately the same critical height but with the fine control rod inserted. This follows the same trend as in the earlier cores.

<u>Table I</u>

Reactor Condition	Critical height (cm)	$\partial\rho/\partial h$ % cm^{-1} From Figure 3	Reactivity change from Clean critical %
Normal (except for experimental fission chambers)	151.03 ± 0.01	0.115	
Pressure tube and contents removed from J10	157.06 ± 0.01	0.108	− 0.67 ± .01
Pressure tube and contents removed from H08	155.79 ± 0.01	0.109	− 0.53 ± .01
Pressure tube and contents removed from H06	155.76 ± 0.01	0.109	− 0.53 ± .01
Fission chamber + Cadmium sleeve 90 cm above tank bottom in K11	151.72 ± 0.01	0.113	− 0.08 ± .01
Coarse control rod fully inserted (see figures 1 and 3)	152.13 ± 0.01	0.114	− 0.13 ± .01
Fine control rod fully inserted (see figures 1 and 3)	156.76 ± 0.01	0.108	− 0.64 ± .01 (0.62 using $\partial\rho/\partial h$ experimental
BF_3 chamber ~ 80 cm above tank bottom placed in K11	151.51 ± 0.01	0.114	− 0.05 ± .01

The effect was large in the first and second core, but barely significant in the fifth core, and it would appear to be larger the greater the magnitude of $\partial\rho/\partial h$. Further theoretical investigation of this effect is clearly necessary.

Table II summarises the measurements of negative reactivities using the sub-critical multiplication technique. Figure 6 shows the counter positions during these measurements.

Table II

Reactivities deduced by sub-critical multiplication measurements

Moderator height (cm)	Fine control rod position	Safety rod positions	Negative reactivities % deduced from counters (see Figure 4) arranged in order of distance from source					
			Ch.I	Ch.III	Log A	Log B	Linear	Mean
151.06	IN	OUT	0.640	0.638	0.654	0.649	0.69	0.655
152.46	IN	OUT	0.480	0.478	0.494	0.490	0.53	0.495
151.06	OUT	Bank A IN	4.9	6.0	8.2	5.0	3.3	5.5
151.06	OUT	Bank B IN	5.0	3.3	3.5	3.5	7.5	4.6
151.06	OUT	Both Banks IN	15.6	11.0	13.9	10.9	12.5	12.8
122,2	OUT	OUT	4.3	5.2	4.5	3.9	4.3	4.4

Examination of Table II and Figure 6 shows that the variation in apparent reactivity follows the same trends as were observed in all earlier experiments (see, in particular, reference (1)). The sub-critical estimate of fine control rod reactivity (0.655%) was in good agreement with the critical estimate (0.64%) of Table I. Due to the obvious limitations of the method the true reactivities and their associated errors are indeterminable; as previously, the most pessimistic individual results were used to satisfy the safety criteria.

5. Macroscopic Reaction Rate Distributions

The measurements were made using U235 and Pu239 fission chambers in precisely the manner as described in reference (1). The radial measurements were made with the active centre of the chambers ~ 75 cm above the tank bottom (~ 55 cm above bottom of fuel) - see Figure 2. Appendix II gives the results in detail and sections 5.1 and 5.2 summarise the spectrum and radial buckling results respectively. The axial measurements were made in the central search tube (K11) and an adjacent one (K13); the results are detailed in Appendix III and summarised in section 5.3. Consistent with the earlier reports (see reference (1) in particular) we have allowed for a 0.1% counter drift error on each counter (0.14% on counts relative to monitor counts) in addition to the Poissonian variation of the number of counts recorded. All measurements have a counter dead time correction of 1.5 ± .5 μsec applied, although count rates were such that the correction was less than 0.5% on each count and in general less than 0.1% on a ratio of counts

5.1 Spectrum results

The plutonium 239 to uranium 238 reaction rate ratio, uranium 235 cadmium ratio (R_5) and plutonium 239 cadmium ratio (R_9) were measured at most available radii inside D_2O - filled search tubes. The results are summarised in Table 1 of Appendix II and plotted against radius in Figure 7. All three parameters were found to be constant, within their estimated errors of $\pm$ .4% out to a radius of 48.3 cm (two lattice pitches), and the results were averaged, giving, for the centre core region:-

$$R_5 = 31.4 \pm .1$$

$$R_9 = 41.5 \pm .5$$

$$\frac{\text{Pu/U DIMPLE}}{\text{Pu/U NESTOR THERMAL COLUMN}} = 1.152 \pm .004$$

This latter result was in good agreement with the value of 1.145 $\pm$ .046 obtained using Pu/Al and U235/Al foils (see section 9).

The results quoted above are uncorrected for attenuation of flux by the chamber wall and active coating, or the effect of displacing D_2O by the fission chamber.

5.2 Radial component of buckling β^2

A summary of all results obtained in the radial scan is presented in Table 2 of Appendix II. As in the earlier cores a statistical analysis was carried out to determine the region of constant spectrum and to check the symmetry of the core.

Examination of Table 2 of Appendix II shows a marked symmetry between the flux ratios in K09 (0.966 $\pm$ 0.001) and K13 (0.974 $\pm$ .002), which are both at radius 24.13 cm from the core centre. Section 5.4 describes a further investigation into this asymmetry. The four results at a larger radius of 48.26 cm i.e. K07 (0.860 $\pm$ .002), K15 (0.854 $\pm$ .001), G11 (0.856 $\pm$ .001) and 011 (0.856 $\pm$ .002) were much more symmetrical

Table 3 of Appendix II gives the results of the computation of radial buckling. The error on β was calculated in precisely the manner of the earlier reports (1), (2), (3). Results are summarised in Table III below, K09 and K13 being treated separately.

Table III

Estimates of β

Position of measurement	Radius (cm)	Value of β (m^{-1})
K09	24.13	1.542 $\pm$ .024
K13	24.13	1.351 $\pm$ .044
K07, K15, G11, 011	48.26	1.604 $\pm$ .009
G13	54.05	1.510 $\pm$ .019

In Table 4 of Appendix II weighted mean values of β, together with the "goodness of fit" parameter χ^2, are tabulated for various combinations of the above results. Examination of Table III above indicates that K13 is in error, and some doubt of the validity of G13 exists since this might be outside the region of constant spectrum illustrated in Figure 7. The final value of β was calculated, neglecting these two positions, to be $1.596 \pm .019\ m^{-1}$, the standard deviation quoted being scaled up to be consistent with the fit of the two values used. On this basis the radial buckling was $2.55 \pm .06\ m^{-2}$, but in view of the asymmetries present it is recommended that the error quoted should be increased by about a factor of two, giving

$$\underline{\beta^2 = 2.55 \pm .12\ m^{-2}}$$

It is interesting to note that, whereas in the H_2O - cooled version of the centre zone [3] the spectrum was apparently constant out to a radius of 72.4 cm, this was not true of this core. This gives further justification to the decision not to use the point at 72.4 cm in computing the radial buckling of core 5.

The radial distributions obtained with the bare and cadmium covered U235 and Pu239 chambers are plotted in Figure 8, together with the deduced $J_0\ (\beta r)$.

5.3 Axial component of buckling

Measurements were made using a 10' long U235 fission chamber, connected to an extension scale, which was moved manually from above the top biological shield in precisely the manner used in earlier cores [1]. Scans were made with cadmium covered and bare chambers in K11, and merely cadmium covered in K13.

The cadmium ratio obtained is plotted in Figure 9. As in the previous core [3], the ratio falls at points near to the centre plate of the 28" long clusters, but rises at the join of the clusters. Figure 3 shows quite clearly that the main difference between the centre and end plates was that the 1.8% (28" long) fuel in the centre 23 pencils was continuous through the centre plate, whereas there was a 2.35 cm gap in the fissile material of the outer twenty pencils in this centre plate. Because of this behaviour only very few points could be fitted to a cosine to produce an estimate of the axial buckling. These points are shown in Figure 10. Table IV below summarises the results, which were corrected where required for the effect of the cadmium covered fission chamber in the manner described in reference (1). The complete experimental scans in search tube K11 (corrected for dead time) divided by the fitted cosine are given in Figure 10, and details of all three scans are given in Appendix III.

Table IV

Results of cosine fitting to axial scans

Position	Type	H	Z_o	χ^2	Degrees of freedom	Probability of χ^2 being exceeded in random sampling	Corrected H
K11	Bare	155.2±0.6	110.0±0.1	1.3	3	60%	
K11	Cd covered	157.8±0.7	110.8±0.1	6.8	3	8%	157.2±0.7
K13	Cd covered	158.0±0.9	110.8±0.1	6.5	3	9%	157.5±0.9

The behaviour of the total and epi-cadmium reaction rates at the ends and centres of the clusters are quite different. Whereas the total reaction rate rises at the end of a 28" cluster, it falls at the end and rises at the centre plate. The major difference between end and centre plate geometry is that only the outer ring of fuel has a gap in the latter whereas all fuel has a gap in the former.

One possible explanation of the observed phenomena would be that removal of moderating coolant but not fuel, (i.e. replacement of coolant by aluminium) causes the epi-cadmium neutron flux to rise and the thermal flux to fall, whereas removal of moderating coolant and fuel causes a nett fall in epithermal flux (because fewer fast neutrons are produced) and a nett rise in thermal flux (since fewer neutrons are absorbed with no fuel present).

Alternatively one could argue that the epi-cadmium peak at the centre plate is associated with the reduction of U238 absorptions in the outer ring (since there is a fuel gap in this ring). At the top plate removal of all fuel removes fast sources and reduces the local epi-cadmium flux, overriding the effect observed in the centre plate. Which, if either, of the above explanations is correct will only be clear after considerable theoretical investigation.

The total perturbation of the epi-cadmium reaction rate was +2% to −2%, and of the total reaction rate was + .8% to −1.4%. Having corrected the cadmium covered scans in the manner recommended in reference (1), the overall mean effective height was calculated by weighting results by the inverse of their deviations from the cosine, and was as follows

$$H = 156.0 \pm 0.6 \text{ cm}$$
$$\alpha = 2.014 \pm .008 \text{ m}^{-1}$$
$$\alpha^2 = 4.06 \pm .03 \text{ m}^{-2}$$

Top extrapolation distance = 8.4 cm
Bottom extrapolation distance = 17.0 cm

combined error ± 0.6 cm

The errors in α^2 quoted above are those deduced from the consistency between one bare and two cadmium covered scans. Due to the extremely limited region used in the fit and the fact (see Figure 8) that there is only a small axial region of constant cadmium ratio, it would be imprudent not to add a large systematic error to the random errors deduced from these measurements. In the absence of any theoretical evidence it is recommended that the value of α^2 to be compared with theory should be $4.1 \pm .3\ m^{-2}$. (i.e. we should arbitrarily increase the error by a factor ten).

5.4 Radial asymmetry in the core

Examination of Table 2 of Appendix II indicates that a noticeable asymmetry of 0.8 ± .2% existed between search tubes K09 and K13 situated at radii of 24.13 cm either side of the core centre. This asymmetry did not, apparently, extend beyond this region. The effect was independent of search tube or fission chamber angular orientation, or the nature of the reaction rate measured.

Just prior to dismantling the core an experiment was carried out to investigate this effect, as follows:-

(a) Two fission chambers were placed, one in each of these search tubes, and a series of counts taken. The fission chambers were reversed and the count repeated.

(b) The search tubes were exchanged and (a) was repeated.

(c) The fission chambers were covered with cadmium sleeves and (a) was repeated.

(d) The 4 pressure tubes complete with fuel surrounding K09 were exchanged for those surrounding K13.

Table V below summarises the results. The errors quoted are due to counting statistics plus 0.1% per count for counter drift.

Table V

State	Ratio of K13/K09	
	Fission chamber 1	Fission chamber 2
a	1.0047 ± .0015	1.0048 ± .0015
b	1.0047 ± .0015	1.0090 ± .0015
c	1.0046 ± .0015	1.0060 ± .0015
d	0.9959 ± .0015	0.9972 ± .0015

Comparison of cases (c) and (d) shows that the effect of exchanging the pressure tubes and contents surrounding one search tube with those from the other reversed the asymmetry. Two independent fission chambers indicated a change in the ratio of .0087 ± .0024 and 0.0082 ± .0024 respectively. Since this change, in both cases, was beyond the 3σ limit (with errors which were overestimated in all probability), we conclude that the asymmetry observed was associated with the fuel clusters and/or the pressure tubes surrounding the two search tubes. The coolant in each pressure tube was analysed for D_2O content and all were found to be within the quoted experimental error of $\pm$ 0.3%. The clusters were examined and found to be visually identical. The pressure tubes were examined for bowing but none was found. Due to shortage of time the investigation was concluded at this point with no obvious reason for the discrepancy apparent.

6. Microscopic reaction rate distributions using manganese foils

One-half inch diameter by 0.005 inch thick manganese foils were placed, in two planes 6.7 cm apart, between fuel pellets in special telescopic fuel pencils, on the outside of the pressure tube, on the inside of the calandria tube, and inside a D_2O filled search tube. Full details of the equipment used for positioning and counting the foils is included in reference 3.

The DIMPLE collapsible foil machine used in the earlier cores was abandoned for this and subsequent experiments (since it was found to give poor foil positional accuracy), and thus only one position in the moderator (that in a search tube) was measured. The foils were positioned accurately in a vertical plane in the search tube by means of a 0.375 inch diameter by .039 inch walled aluminium tube; accurate height registration was given by slots in this tube at its lower end. Around the foils the tube was extensively cut away to reduce the amount of aluminium/unit length to about 20% of normal.

Three irradiations, each with two layers of foils in planes 52.4 and 59.1 cm above the bottom of the fuel, were carried out. Examination of Figure 10 shows that the foils were in the region of constant spectrum between the centre plate and top of the lower 28 inch cluster.

Appendix IV gives details of the irradiations in Table 1 and a summary of the results is given in Table 2. Standard deviations were computed from the run-to-run consistency in Table 2 in the manner described in reference 1, and were between 1 and 2% depending on the position of the foil. The results are plotted in Figure 11.

All three irradiations were carried out with the foils placed on a radius from the centre of the reactor passing through the centre of the fuel element J10 (see Figure 1). For the first two irradiations foils were placed between the centre of J10 and the core centre. In the third irradiation the pressure tube was rotated through 180 degrees and the foils were placed (still in J10) between the centre of J10 and the centre of H8. Thus the macroscopic corrections $^1/J_0(\beta r)$ [r is the radius of the foil from the core centre] applied were different in this third irradiation and the first two irradiations. Examination of Table 2 of Appendix IV shows no systematic differences between these irradiations outside the experimental errors of $\pm$ 1%. Thus it would appear that the procedure of making a macroscopic correction is valid within the precision of these results.

7. Microscopic reaction rate ratios using Indium foils

Two irradiations were carried out, each with a single layer of foils, in the fuel and moderator only. Results are given in detail in Appendix V Table I, summarised in Appendix V Table II, and plotted, together with the manganese results, in Figure 11.

8. Luteoium to manganese reaction rate ratios in the lattice cell

Three irradiations were carried out using foils from the same batch as were used in the previous core (reference 3). The technique was unaltered from reference 3, and results are given in detail in Appendix VI. As before, the manganese activity was separately analysed (Tables 3 and 4) and plotted in Figure 11. The agreement between these measurements and the manganese measurements was very satisfactory. The luteoium to manganese ratio is given in detail in Table 1 of Appendix VI, summarised in Table 2, and plotted in Figure 12. Run-to-run consistency was within the errors of $\pm$ 2 % estimated in the analysis of results from the activity counting.

9. Plutonium to uranium reaction rate ratios in the lattice cell

Two irradiations were carried out in lattice cell J10 using plutonium 239-aluminium and uranium 235-aluminium foils. The experiment was carried out in an identical manner to that described in reference 3. Detailed results are recorded in Appendix VII Table 1, and are summarised in Appendix VII Table 2.

Examination of these results indicated that the errors produced by analysis of the counting sequence (those quoted in Table I are based on the consistency of the counts obtained during the experiment) were quite insufficient to explain the differences in ratios of up to 10 % obtained in separate irradiations. Up to that point in time the importance of placing the wrapped plutonium foils the same way up in the counting equipment has not been appreciated. A subsequent experiment showed that about a 3% difference existed between results counted one way up and the reverse way due to the foil overlap on one side produced by the wrapping process. This 3% error goes some way to explaining the observed discrepancies between irradiations. Results obtained in later cores, where careful note of the foil orientation was made, point to this as being the most probable explanation.

Results from both irradiations are averaged in Table 2, and the error on the mean at each position computed from the average range of the two irradiations. The results are plotted in Figure 13.

10. Uranium 238 to uranium 235 Fission Ratio and Relative Conversion Ratio

The technique has been fully described in references 4 and 5 and its application to DIMPLE is described in the previous report in this series (Reference 3).

Three irradiations were carried out, and the results are given in Appendix VIII. The chemical separation technique was not used in this core. In Appendix VIII Table 1 gives details of individual runs, and Table 2 summarises the RCR and fission ratio results which are plotted in Figure 14. Finally Table 3 of Appendix VIII gives the results of U238 capture, U235 fission, and U238 fission in each ring of fuel, and these are plotted in Figure 15. The sharp rise of the U238 fission rate in the outer ring of fuel pencils compared with the smoother variation of U235 fission (see Figure 15) explains the somewhat discontinuous variation of the U238 to U235 fission ratio (see Figure 13).

There are three types of error associated with the RCR and fission ratio results of Appendix VIII, namely

(1) Estimated errors, based on run-to-run consistency of results.

(2) Relative errors, which are calculated from the estimated errors plus foil holder calibration errors.

(3) Total errors, which are calculated from the relative errors plus known sources of systematic errors.

For the RCR measurements a correction of + 3.7% to the measured value was necessary to correct the DIMPLE reference spectrum to that in NESTOR. The method of making this correction by measuring the U238 cadmium ratio in the reference search tube (C15) introduced a systematic error of up to -2%, that is, the correction of + 3.7% might be too large by up to 2%. In addition a correction of up to - 1% (for 2.5 Co) and - 0.3% (1.28 Co) was applied in the RCR to allow for the experimental foils being respectively .010" and .004" smaller in diameter than the normal fuel pellets. The smaller diameter was necessary to allow the experimental foil packs to be wrapped in aluminium foil to ensure alignment. The systematic error due to this effect was ± .2%. Finally a systematic error of - 0.3% allowed for the bowing of the depleted (metal) foils used in the fission ratio, since the fission ratio result was fed into the RCR calculation.

For the fission ratio measurements a systematic error of ± 10% arises from the uncertainty in the calibration factor relating fission product activity ratio to actual fission ratio.

11. Conclusions

(1) Poorer spectral matching between centre (D_2O/H_2O mixture cooled) and driver (H_2O cooled) regions in this core compared with the fifth core (3) (where both regions were H_2O cooled) has reduced the radial region of constant cadmium ratio to 48.3 cm or slightly greater. This is, however, still considerably greater than that of the first two cores (1), (2). The radial component of buckling was deduced to be 2.55 ± .12 m^{-2}, the error quoted being double the random error to allow for systematic effects caused by the known, but little understood, asymmetry.

(2) An unmistakable radial asymmetry existed in the centre of the core. This was shown to be a function of the fuel surrounding the relevant search tubes, but examination of the fuel and coolant revealed no obvious cause. An axial scan in the relevant search tube agreed well with another in the core centre.

(3) The axial flux shape was once again seriously perturbed by the gaps in the fuel and the presence of aluminium spacer plates, and only six measuring positions out of twenty six were used in the final fit, since the regions of apparently constant spectrum between plates (themselves about 30 cm apart) was 10 cm or less. The axial component of buckling was deduced to be 4.06 ± 0.03 m^{-2}, the standard deviation quoted being based on internal consistency only. It is recognised that the method of analysis used cannot eliminate entirely the possibility of some systematic error, and for this reason we have arbitrarily increased the above error by a factor of ten in our recommendation.

(4) Internal consistency of microscopic reaction rate distributions were very satisfactory with the one exception of the plutonium to uranium ratio. It is thought that the poor consistency here was mainly due to non-appreciation of the importance of counting the foils with one particular face upwards, since the method of foil wrapping was not uniform on both sides of the foil.

(5) During the manganese microscopic reaction rate measurements it was demonstrated that macroscopic correction to the observed reaction rates by $1/J_0(\beta r)$ yields consistent results when the macroscopic correction to be applied differs appreciably between irradiations.

(6) Application of experience gained on earlier cores with respect to detector positioning has improved the shape of the approach-to-critical curves and reduced the differences between estimates of reactivity by the sub-critical mulitplication technique.

Acknowledgements

The Authors wish to acknowledge the co-operation of the DIMPLE Operations and Maintenance Staff, without whose efforts much of the work reported here could never have been completed in the time allotted (the experiment was completed in two and a half weeks).

References

(1) AEEW - M 309 The first core in Dimple at A.E.E. Winfrith - Experimental results - A. G. Collins, W. H. Taylor, G. M. Wells.

(2) AEEW - M 310 The second core in DIMPLE at A.E.E. Winfrith - Experimental results - A. G. Collins, R. E. B. Strathen, W. H. Taylor, G. M. Wells.

(3) AEEW - M 311 The fifth core in DIMPLE at A.E.E. Winfrith - Experimental results - W. A. V. Brown, A. G. Collins, W. H. Taylor, G. M. Wells.

(4) AEEW - R 340 Measurement of relative conversion ratio - W. A. V. Brown and D. J. Skillings (in course of publication).

(5) AEEW - R 341 Measurement of fast fission ratio - W. A. V. Brown and D. J. Skillings (in course of publication).

Appendix I

Details of core materials

The details were identical to those of reference 3 with the one exception that, for region A (see Figure 4 (b) of this report), the H_2O was replaced by a mixture of 29.7% H_2O and 70.3% D_2O by weight.

Reference 3 should be used to obtain all necessary data.

Appendix II

Radial scan results

Table 1

Spectrum results

Pitch radius	Radius (cm)	Search tube position	Pu239/U235 ratio value	% SD	R_5 normalised to K11 value	% SD	R_9 normalised to K11 value	% SD
0	0	K11	.4032	.3	1.000	.3	1.000	.4
1	24.13	K09	.4043	.4	0.997	.3	1.003	.4
		K13	.4052	.4	1.011	.3	0.999	.4
2	48.26	K07					1.002	.4
		K15	.4042	.4	1.006	.3	1.010	.4
		G11	.4061	.4	0.996	.3	0.996	.4
		O11	.4054	.4	1.004	.3	1.000	.4
$\sqrt{5}$	54.05	G13	.4023	.4				
3	72.39	K17	.3981	.4	1.141	.4	1.117	.5
4	96.52	K19	.3756	.4	2.264	.4	2.123	.5

Absolute R_5 in K11 = 31.4 ± .1
Absolute R_9 in K11 = 41.5 ± .5
Mean Pu/U ratio (out to radius of 48.5 cm) = 0.4047 ± .0006
Pu/U ratio in NESTOR Thermal column (reference 1) = 0.3514 ± .0009
Pu/U DIMPLE/Pu/U NESTOR = 1.152 ± 0.004

(compared with 1.145 ± .046 using Pu and U foils – see Appendix VII)

Table 2

Summary of all radial scan results

Pitch Radius	Radius (cm)	Search tube position	Ratios to K11																			
			U235 Bare								Pu Bare	Mean of all Bare	S.D. on mean	U under Cd	Pu under Cd	Mean of all U/C	S.D. on mean	Overall mean	S.D.	Radius mean	S.D.
			Individual measurements						Mean	S.D. on mean											
0	0	K11	1.0000 0.9985	1.0000	1.0000	1.0000	1.0000 1.0019	1.0000 1.0018	1.00025		1.0000 1.0023	1.00041		1.0000 1.0017		1.00085	–	1.00047		1.00047	
1	24.13	K09	0.9627	0.9659	0.9653		0.9679	0.9687	.9661	.00104	0.9663	.9662	.00084	0.9676	0.9610	.9643	–	0.9657	0.0009	0.9701	$\frac{0.0013}{\sqrt{2}}$
		K13	0.9742	0.9692		0.9758	0.9732 0.9751	0.9672 0.9775	.9732	.0014	0.9801	.9740	.0015	0.9648	0.9788	.9718	–	0.9736	0.0016		
2	48.26	K07			0.8638		0.8563	0.8599	0.8600	0.0022	0.8617	0.8604	0.0016		0.8577	0.8577	–	0.8599	0.0014	0.8557	$\frac{0.0008}{\sqrt{1.47}}$
		K15	0.8539	0.8559		0.8586	0.8542	0.8548	0.8555	0.0009	0.8570	0.8557	0.0007	0.8507 0.8501	0.8578 0.8468	0.8557	–	0.8540	0.0012		
		G11	0.8549		0.8554	0.8523	0.8527		0.8538	0.0008	0.8582	0.8547	0.0011	0.8525 0.8600	0.8636	0.8587	–	0.8562	0.0014		
		O11	0.8526			0.8584		0.8592	0.8567	0.0021	0.8621	0.8580	0.0020	0.8503	0.8560	0.8531	–	0.8564	0.0018		
$\sqrt{5}$	54.05	G13	0.8408		0.8415				–	–	0.8399	0.8407	0.0005	–	–	–	–			0.8407	0.0005
3	72.39	K05			0.7164				–	–		0.7164								Bare 0.7211 U/C 0.6337	0.0021 –
		K17	0.7199	0.7216					–	–	0.7117	0.7177		0.6320	0.6355	0.6337	–				
		E11				0.7266			–	–		0.7266									
4	96.52	K03		0.6016					–	–											
		K19	0.6252 0.6219	0.6266	0.6247				–	–	0.5846			0.2767	0.2748	0.2758					
		C11				0.6298			–	–											
		% error	.3	.4	.4	.4	.3	.3			.4			.4	.4						

Table 3

Radial buckling

Position	Radius (cm)	ϕ	Var ϕ	β	Var β	S.D. β	$^1/$Var β
K11	0	1.0000	–	–	–	–	
K09	24.13	0.9657	0.8×10^{-6}	1.542	5.5×10^{-4}	0.024	1.82×10^{3}
K13	24.13	0.9736	2.6×10^{-6}	1.351	18.7×10^{-4}	0.044	0.53×10^{3}
K07,K15,G11,O11	48.26	0.8557	0.9×10^{-6}	1.604	0.8×10^{-4}	0.009	12.50×10^{3}
G13	54.05	0.8407	13.0×10^{-6}*	1.510	3.5×10^{-4}	0.019	2.86×10^{3}

*Based on theoretical error of 0.4% on each of three measurements increased by factor 2 to all allow for possible asymmetry.

Table 4

Measurements used	$\bar{\beta}$	Var $\bar{\beta}$	x^2	Corrected S.D. on $\bar{\beta}$
All	1.575	0.6×10^{-4}	51	.032
All except K13	1.582	0.6×10^{-4}	24	.027
All except K13 and G13	1.596	0.6×10^{-4}	5.7	.019

Appendix III

Axial scan results

Chamber Position Z (cm)	U235 Bare fission chamber in K11 A = 1.5446, H = 155.159, Z_o = 110.999, x^2 = 1.3				U235 Cadmium covered fission chamber in K13 A = 0.0502, H = 157.802, Z_o = 110.833, x^2 = 6.8				U235 Cadmium covered fission chamber in K13 A = 0.04793, H = 158.027, Z_o = 110.778, x^2 = 6.6			
	ϕobs [corrected for dead time]	ϕcalc. $\left[A\cos\frac{\Pi}{H}(Z-Z_o)\right]$	$\frac{\phi obs}{\phi calc.}$	x^2 [fitted points only]	ϕobs	ϕcalc.	$\frac{\phi obs}{\phi calc.}$	x^2	ϕobs	ϕcalc.	$\frac{\phi obs}{\phi calc.}$	x^2
170	0.58121	0.56742	1.0243		0.01805	0.01923	0.939		0.01725	0.01838	0.939	
165	0.66223	0.70971	0.9331		0.02194	0.02375	0.924		0.02103	0.02268	0.927	
160	0.83427	0.84473	0.9876		0.02728	0.02803	0.973		0.02584	0.02676	0.966	
155	0.97139	0.97111	1.0003	.007	0.03197	0.03203	0.998	0.23	0.03045	0.03057	0.996	0.70
150	1.08743	1.08754	0.9999	.001	0.03577	0.03572	1.002	0.16	0.03421	0.03408	1.004	0.79
145	1.19235	1.19280	0.9996		0.03927	0.03905	1.006		0.03786	0.03726	1.016	
140	1.26610	1.28587	0.9846		0.04279	0.04199	1.019		0.04066	0.04006	1.015	
135	1.34792	1.36577	0.9869		0.04502	0.04453	1.011		0.04309	0.04248	1.014	
130	1.41456	1.43169	0.9880		0.04696	0.04662	1.007		0.04524	0.04447	1.017	
125	1.48481	1.48295	1.0013		0.04863	0.04825	1.008		0.04662	0.04603	1.013	
120	1.51556	1.51905	0.9977	0.662	0.04963	0.04939	1.005	2.38	0.04734	0.04713	1.004	1.49
115	1.54299	1.53957	1.0022	0.619	0.04985	0.05005	0.996	1.88	0.04756	0.04776	0.996	1.38
110	1.55344	1.54428	1.0059		0.04974	0.05022	0.990		0.04785	0.04792	0.999	
105	1.54591	1.53322	1.0083		0.04920	0.04989	0.986		0.04738	0.04761	0.995	
100	1.51837	1.50645	1.0079		0.04808	0.04907	0.980		0.04603	0.04683	0.983	
95	1.47235	1.46426	1.0055		0.04677	0.04776	0.979		0.04456	0.04559	0.977	
90	1.41704	1.40708	1.0071		0.04524	0.04597	0.984		0.04365	0.04390	0.994	
85	1.33617	1.33552	1.0005	0.027	0.04357	0.04375	0.996	1.17	0.04159	0.04177	0.996	1.19
80	1.24954	1.25024	0.9994	0.033	0.04120	0.04106	1.003	0.98	0.03939	0.03923	1.004	1.01
75	1.14600	1.15214	0.9947		0.03805	0.03798	1.002		0.03683	0.03631	1.014	
70	1.03178	1.04228	0.9899		0.03454	0.03453	1.000		0.03349	0.03302	1.014	
65	0.90844	0.92173	0.9856		0.03116	0.03073	1.014		0.02956	0.02941	1.005	
60	0.78069	0.79174	0.9860		0.02675	0.02663	1.005		0.02581	0.02551	1.011	
55	0.64500	0.65366	0.9868		0.02231	0.02227	1.002		0.02128	0.02136	0.996	
50	0.49439	0.50888	0.9715		0.01770	0.01768	1.001		0.01669	0.01700	0.982	
45	0.32089	0.35888	0.8941		0.01233	0.01292	0.954		0.01203	0.01247	0.965	

Appendix IV

Manganese foil irradiation results

Table 1

Basic Results

Details of irradiation

Run No:- I *Note incorrectly placed foil - macroscopic correction includes axial factor
Date:- 13/11/62.
Axial foil positions:- 59.14 cms and 52.44 cms above bottom of fuel.

Foil Position	Radius from cell centre (CM)	Radius from core centre (CM)	Foil No.	Activity (arbitrary) units	Foil calibration factor	Corrected activity (for each factor)	Macro-scopic correction factor	Final corrected activity I (normalised to centre foil)
59.14	0	17.062	21	54485	1.0247	53172	0.98464	0.25594
59.14	1.803	15.259	7	61998	1.1000	56362	0.98778	0.27043
59.14	3.708	13.354	18	76619	1.0543	72673	0.99063	0.34752
59.14	5.525	11.537	2	118477	1.0957	108125	0.99299	0.51607
59.14	6.993	10.069	4	161469	1.0054	160601	0.99464	0.76527
59.14	7.931	9.131	3	174855	1.0927	160021	0.99559	0.76178
75.94	15.662	1.40	16	220245	1.1008	200077	0.94826*	1.00000
52.44	0	17.062	11	52556	0.9911	53028	0.98464	0.24316
52.44	1.803	15.259	23	56161	0.9987	56234	0.98778	0.25704
52.44	3.708	13.354	10	71179	1.0121	70328	0.99063	0.32054
52.44	5.525	11.537	1	106740	0.9943	107351	0.99299	0.48812
52.44	6.993	10.069	5	154655	1.0670	144943	0.99464	0.65795
52.44	7.931	9.131	19	163504	1.0405	157140	0.99559	0.71264
52.44	17.062	0	26	239333	1.0806	221481	1.00000	1.00000

Table 1 (contd.)

Basic Results

Details of irradiation

Run No:- II
Date:- 14/11/62.
Axial foil positions:- 59.14 cms and 52.44 cms above bottom of fuel

Foil Position	Radius from cell centre (CM)	Radius from core centre (CM)	Foil No.	Activity (arbitrary) units	Foil calibration factor	Corrected activity (for each factor)	Macro-scopic correction factor	Final corrected activity I (normalised to centre foil)
59.14	0	17.062	24	25040	0.9994	25055	0.98464	0.24807
59.14	1.803	15.259	32	25937	0.9860	26305	0.98778	0.25962
59.14	3.708	13.354	22	35909	1.0864	33053	0.99063	0.32528
59.14	5.525	11.537	25	53796	1.0709	50234	0.99299	0.49319
59.14	6.993	10.069	8	74823	1.0342	72349	0.99464	0.70913
59.14	7.931	9.131	14	75075	0.9966	75331	0.99559	0.73765
59.14	16.562	0.50	27	102163	0.9960	102573	0.99998	1.00000
52.44	0	17.062	17	26215	1.0731	24429	0.98464	0.24651
52.44	1.803	15.259	29	28044	1.0887	25759	0.98778	0.25911
52.44	3.708	13.354	31	32350	0.9912	32637	0.99063	0.32735
52.44	5.525	11.537	13	54814	1.1137	49218	0.99299	0.49248
52.44	6.993	10.069	28	71044	0.9905	71725	0.99464	0.71650
52.44	7.931	9.131	20	80348	1.0891	73775	0.99559	0.73628
52.44	17.062	0	15	105073	1.0440	100644	1.00000	1.00000

Table 1 (contd.)

Basic Results

Details of irradiation

Run No:- III
Dates:- 16/11/62.
Axial foil positions:- 59.14 cms and 52.44 cms above bottom of fuel

Foil Position	Radius from cell centre (CM)	Radius from core centre (CM)	Foil No.	Activity (arbitrary) units	Foil calibration factor	Corrected activity (for each factor)	Macro-scopic correction factor	Final corrected activity I (normalised to centre foil)
59.14	0	17.062	28	27206	0.9905	27467	0.98464	0.25535
59.14	1.803	18.865	24	28010	0.9994	28027	0.98114	0.26149
59.14	3.708	20.710	32					
59.14	5.525	22.587	16	58181	1.1008	52853	0.97310	0.49718
59.14	6.993	24.055	29	82770	1.0887	76026	0.96958	0.71776
59.14	7.931	24.993	22	85160	1.0864	78387	0.96718	0.74189
59.14	17.312	0.50	5	116561	1.0670	109242	0.99998	1.00000
52.44	0	17.062	18	28809	1.0543	27325	0.98464	0.24903
52.44	1.803	18.865	26	30362	1.0806	28097	0.98114	0.25698
52.44	3.708	20.770	19		1.0405			
52.44	5.525	22.587	25	65390	1.0709	52257	0.97310	0.48191
52.44	6.993	24.055	27	74050	0.9960	74347	0.96958	0.68810
52.44	7.931	24.993	23	77148	0.9987	77248	0.96718	0.71673
52.44	17.062	0	2	122101	1.0957	111436	1.00000	1.00000

Table 2

Summary of results

$\bar{C}_{i1}$ = Mean ratio of activity in run i to that in run 3 in each position measured.

$\bar{C}_{11} = 0.95265$ $\bar{C}_{21} = 1.01508$ $\bar{C}_{31} = 1.00000$ $\bar{C}_{41} = 0.99928$ $\bar{C}_{51} = 0.98976$ $\bar{C}_{61} = 1.01202$

Radius from cell centre (cm)	$x_1 \bar{C}_{11}$	$x_2 \bar{C}_{21}$	$x_3 \bar{C}_{31}$	$x_4 \bar{C}_{41}$	$x_5 \bar{C}_{51}$	$x_6 \bar{C}_{61}$	Mean	Standard Deviation
0	0.24382	0.24683	0.24807	0.24633	0.25202	0.24830	0.24830	0.0010
1.803	0.25763	0.26092	0.25962	0.25892	0.25881	0.26007	0.25933	0.0010
3.708	0.33106	0.32537	0.32528	0.32711			0.32721	0.0012
5.525	0.49163	0.49548	0.49319	0.49213	0.49209	0.48770	0.49204	0.0010
6.993	0.72903		0.70913	0.71598	0.71041	0.69637	0.71218	0.0039
7.931	0.72571	0.72339	0.73765	0.73575	0.73429	0.72535	0.73036	0.0036
17.062		1.01508	1.00000	0.99928	0.98976	1.01202	1.00323	0.0015

Remarks:

The omissions in columns x_1 and x_2 were results which differed from the mean by 6 standard deviations, probably arising through foil positioning errors.

Appendix V

Table 1

Basic Results

Details of irradiation

Run No:- I
Date:- 15/11/62.
Axial foil positions:- 49.54 cms above bottom of fuel

Foil Position (cms)	Radius from cell centre (CM)	Radius from core centre (CM)	Foil No.	Activity (arbitrary) units	Foil calibration factor	Corrected activity (for each factor)	Macro-scopic correction factor	Final corrected activity x (normalised to centre foil)
49.54	0	17.062	219	45907	1.0074	45570	0.98464	0.42321
49.54	1.803	15.259	203	49298	0.9352	52658	0.98778	0.48749
49.54	3.708	13.354	208	56686	1.0413	54438	0.99063	0.50251
49.54	5.525	11.537	216	65140	0.9435	69041	0.99299	0.63580
49.54	17.062	0	202	109356	1.0000	109356	1.00000	1.00000

Table 1 (contd.)

Basic Results

Details of irradiation

Run No:- II
Date:- 14/11/62.
Diagram:- See Fig.
Axial foil positions:- 52.44 cms above bottom of fuel

Foil Position (cms)	Radius from cell centre (CM)	Radius from core centre (CM)	Foil No.	Activity (arbitrary) units	Foil calibration factor	Corrected activity (for each factor)	Macro-scopic correction factor	Final corrected activity I (normalised to centre foil)
52.44	0	17.062	203	20705	0.9352	22140	0.98464	0.45791
52.44	1.803	15.259	202	22422	1.0000	22422	0.98778	0.46227
52.44	3.708	13.354	219	25650	1.0074	25462	0.99063	0.52344
52.44	5.525	11.537	208	32172	1.0413	30896	0.99299	0.63308
52.44	17.062	0	210	48883	0.9955	49104	1.00000	1.00000

Table 2

Summary of results

C_{21} = Mean ratio of activity to run 2 to that in run 1 for each position measured.

= 0.98862

Radius from cell centre (cm)	$x_1 \overline{C}_{11}$	$x_2 \overline{C}_{21}$	Mean	Standard Deviation
0	0.42321	0.45270	0.43796	0.0087
1.803	0.48749	0.45701	0.47225	0.0087
3.708	0.50251	0.51748	0.51000	0.0087
5.525	0.63580	0.62588	0.63084	0.0087
17.062	1.00000	0.98862	0.99431	0.0057

Appendix VI

Manganese/Lutecium foil irradiation results

Table 1

Basic Results

Run No:-	I	II	III
Date of irradiation:-	13/11/62.	15/11/62.	16/11/62.
Time of start of irradiation:-	19 Hrs. 15 M. 21 Secs.	14 Hrs. 18 M. 48 Secs.	8 Hrs. 38 M. 5 Secs.
Length of irradiation:-	1 Hr. 0 M. 8 Secs.	60 Mins.	60 Mins.
Time of start of Mn counting:-	20 Hrs. 53 M. 4 secs. on 13-11-62.	17 Hrs. 23 M. 20 Secs. on 15-11-62.	10 Hrs. 43 M. 45 Secs. on 16-11-62.
Time of start of Lu counting:-	12 Hrs. 42 M. 22 Secs. on 16-11-62.	9 Hrs. 53 M. 1 Sec. on 19-11-62.	11 Hrs. 41 M. 9 Secs. on 19-11-62.
Foil details:-	Dia. 0.480"	Lu content 13.74% by weight	
		Mn content 5.76% by weight	

Run No.	Foil position above bottom of fuel (cms)	Radius from cell centre	Foil No.	Mass (gm)	Mn saturation activity	Lu saturation activity	Lu/Mn saturation activity	Mass correction factor	Corrected Lu/Mn	Lu/Mn in NESTOR	Ratio of core of NESTOR
I	52.5	0	62	0.37008	133590	756097	5.660 ± .093	1.1025	6.2402 ± .1025	5.2277 ± .0128	1.1937
I	52.5	1.803	63	0.37389	142107	826404	5.815 ± .092	1.1035	6.4169 ± .1015	5.2277 ± .0128	1.1227
I	52.5	3.708	64	0.40956	193831	1094471	5.647 ± .079	1.1105	6.2710 ± .0880	5.2277 ± .0128	1.1996
I	52.5	5.525	65	0.36110	261670	1414577	5.406 ± .069	1.1005	5.9496 ± .0760	5.2277 ± .0128	1.1380
I	52.5	17.062	66	0.36836	525058	2624499	4.998 ± .053	1.1021	5.5083 ± .0580	5.2277 ± .0128	1.0537
II	49.54	0	67	0.41855	144420	818516	5.668 ± .087	1.1109	6.2966 ± .097	5.2277 ± .0128	1.2045
II	49.54	1.803	68	0.39148	144528	828925	5.735 ± .088	1.1070	6.3486 ± .097	5.2277 ± .0128	1.2144
II	49.54	3.708	69	0.36380	172188	968442	5.624 ± .080	1.1010	6.1920 ± .088	5.2277 ± .0128	1.1845
II	49.54	5.525	70	0.36912	260925	1399934	5.365 ± .065	1.1012	5.9079 ± .072	5.2277 ± .0128	1.1301
II	49.54	17.062	71	0.37846	540198	2690806	4.981 ± .048	1.1041	5.4995 ± .053	5.2277 ± .0128	1.0520
III	49.54	0	72	0.41273	144602	845135	5.845 ± .088	1.1115	6.4967 ± .098	5.2277 ± .0128	1.2428
III	49.54	1.803	73	0.37234	140235	813190	5.799 ± .089	1.1028	6.3951 ± .098	5.2277 ± .0128	1.2233
III	49.54	3.708	74	0.39326	184012	1054762	5.732 ± .079	1.1071	6.3459 ± .088	5.2277 ± .0128	1.2139
III	49.54	5.525	75	0.34001	246565	1334184	5.411 ± .068	1.1071	5.9332 ± .075	5.2277 ± .0128	1.1135
III	49.54	17.062	76	0.39080	560085	2847794	5.085 ± .051	1.1070	5.6291 ± .057	5.2277 ± .0128	1.0768

Table 2

Summary of results relative to the NESTOR Thermal Column

Lu/Mn ratios

Foil Position	Radius from cell centre	Run No. I	Run No. II	Run No. III	Mean Ratio	Standard Deviation
	0	1.1937 ± 0.0198	1.2045 ± 0.0188	1.2428 ± 0.0190	1.2137	0.0111
	1.803	1.2275 ± 0.0196	1.2144 ± 0.0187	1.2233 ± 0.0190	1.2217	0.0110
	3.708	1.1996 ± 0.0168	1.1845 ± 0.0171	1.2139 ± 0.0170	1.1993	0.0098
	5.525	1.1380 ± 0.0148	1.1301 ± 0.0141	1.1350 ± 0.0146	1.1344	0.0084
Moderator	17.062	1.0537 ± 0.0114	1.0520 ± 0.0105	1.0768 ± 0.0113	1.0608	0.0064

Table 3

Basic Results from the manganese activity

Run No.	I	II	III
Date of irradiation:-	13/11/62.	15/11/62.	16/11/62.
Foil details:- Dia:-	0.480" Lu content 13.74% Mn content 5.76%		
Axial foil positions:-	52.5 cms	49.54 cms	49.54 cms

Run No.	Foil position above bottom of fuel	Radius from cell centre (cms)	Radius from core centre (cms)	Foil No.	Mass (gms)	Mn saturation activity	Mass corrected	Macroscopic correction factor	Final corrected activity X (normalised to centre foil)
I	52.5	0	17.062	62	0.37004	133590	361015	0.98464	0.25722
I	52.5	1.803	15.259	63	0.37359	142107	380077	0.98778	0.26995
I	52.5	3.708	13.354	64	0.40956	193831	473266	0.99063	0.33517
I	52.5	5.525	11.537	65	0.36110	261670	724647	0.99299	0.51197
I	52.5	17.062	0	66	0.36836	525058	1425394	1.00000	1.00000
II	49.54	0	17.062	67	0.41855	144420	345048	0.98464	0.24551
II	49.54	1.803	15.259	68	0.39148	144528	369184	0.98778	0.26185
II	49.54	3.708	13.354	69	0.36380	172188	473304	0.99063	0.33473
II	49.54	5.525	11.537	70	0.36912	260925	706884	0.99299	0.49874
II	49.54	17.062	0	71	0.37846	540198	1427358	1.00000	1.00000
III	49.54	0	17.062	72	0.41273	144602	350355	0.98464	0.24827
III	49.54	1.803	15.259	73	0.37234	140235	376632	0.98778	0.26605
III	49.54	3.708	13.354	74	0.39326	184012	467914	0.99063	0.32958
III	49.54	5.525	11.537	75	0.34001	246565	725170	0.99299	0.50956
III	49.54	17.062	0	76	0.39080	560085	1433176	1.00000	1.00000

Table 4

Summary of results of Manganese activity

$\overline{C}_{i1}$ = Mean ratio of activity in run i to that in run 1 for each position measured.

$\overline{C}_{21}$ = 1.02129 $\overline{C}_{31}$ = 1.01448

Foil position	Radius from cell centre (cm)	$x_1\ \overline{C}_{11}$	$x_2\ \overline{C}_{21}$	$x_3\ \overline{C}_{31}$	Mean	Standard Deviation
52.5	0	0.25722	0.25074	0.25186	0.25327	0.0019
52.5	1.803	0.26995	0.26742	0.26990	0.26909	0.0019
52.5	3.708	0.33517	0.34186	0.33435	0.33713	0.0019
52.5	5.525	0.51197	0.52287	0.51694	0.51726	0.0019
52.5	17.062	1.00000	1.02129	1.01448	1.01192	0.0063

Appendix VII

Plutonium/uranium foil irradiation results

Table 1

Basic results

Run No. 1	In Dimple	In Nestor Thermal Column
Date of irradiation	14/11/62.	11/12/62.
Time of start of irradiation	13.32 hrs.	15.00 hrs.
Length of irradiation	30 mins.	30 mins.
Time of start of counting	15.09 hrs.	16.33 hrs.

Axial height off tank bottom (cm)		Radius from cell centre (cm)	Counter No.	Pu/U ratio		$\frac{\text{Pu/U Dimple}}{\text{Pu/U Nestor}}$	Axial correction factor	Corrected $\frac{\text{Pu/U Dimple}}{\text{Pu/U Nestor}}$
Pu	U			DIMPLE	NESTOR			
72.5	79.2	0	1	1.5832 ± 0.0097	1.1941 ± 0.0048	1.3259	1.0194	1.352 ± 0.007
72.5	79.2	1.803	2	2.0058 ± 0.0103	1.4184 ± 0.0046	1.4141	1.0194	1.442 ± 0.006
72.5	79.2	3.708	3	1.8477 ± 0.0110	1.3592 ± 0.0044	1.3594	1.0194	1.386 ± 0.007
73.0	79.7	5.525	5	1.8180 ± 0.0078	1.4811 ± 0.0108	1.2275	1.0194	1.251 ± 0.014
72.5	79.2	17.062	6	1.5255 ± 0.0059	1.3446 ± 0.0041	1.1346	1.0194	1.157 ± 0.050

Table 1 (contd.)

Run No.	In Dimple	In Nestor Thermal Column
Date of irradiation	15/11/62.	6/12/62.
Time of start of irradiation	12.00 hrs.	14.39 hrs.
Length of irradiation	30 mins.	30 mins.
Time of start of counting	14.12 hrs.	16.47 hrs.

Axial height off tank bottom (cm)		Radius from cell centre (cm)	Counter No.	Pu/U ratio		$\frac{\text{Pu/U Dimple}}{\text{Pu/U Nestor}}$	Axial correction factor	Corrected $\frac{\text{Pu/U Dimple}}{\text{Pu/U Nestor}}$
Pu	U			DIMPLE	NESTOR			
76.4	69.7	0	1	2.0920 ± 0.0142	1.3360 ± 0.0330	1.5660	0.9762	1.529 ± 0.026
76.4	69.7	1.803	2	2.2550 ± 0.0390	1.5232 ± 0.0400	1.4805	0.9762	1.445 ± 0.031
76.4	69.7	3.708	3	1.9698 ± 0.0081	1.4880 ± 0.0180	1.3238	0.9762	1.292 ± 0.013
75.5	69.7	5.525	5	1.9498 ± 0.0083	1.6157 ± 0.0470	1.2068	0.9791	1.182 ± 0.027
69.7	76.4	17.062	6	1.4758 ± 0.0063	1.3337 ± 0.0190	1.0243	1.0243	1.133 ± 0.015

Table 2

Summary of results

Radius from cell centre (cm)	Corrected Pu/U Dimple / Pu/U Nestor			
	Run 1	Run 2	Mean	Error on mean*
0	1.352 ± .007	1.529 ± .026	1.441	0.046
1.803	1.442 ± .006	1.445 ± .031	1.443	0.046
3.708	1.386 ± .007	1.292 ± 0.013	1.339	0.046
5.525	1.251 ± .014	1.182 ± .027	1.217	0.046
17.062	1.157 ± .050	1.133 ± .015	1.145	0.046

*From spread of results mean range = .0734

∴ Mean S.D. = .0734/1.13 = .0649

S.D. on mean of 2 observations $= \frac{.0649}{\sqrt{2}} = .046$

Appendix VIII Relative modified conversion ratio (RCR*) and fission ratio results

TABLE 1 Basic Results

Run No.: D5

Date irradiation: 12/11/62

Time of start of irradiation: 12.33 hours

Length of irradiation: 2 hours

Location of thermal foil: DIMPLE reflector (SEARCH TUBE C.15) U^{238} Cd. Ratio = 27.9

Height correction depleted foil: -0.21%

Remarks: Foil rotator in C15 stopped during the irradiation

Radius from cell centre (cm)	Rel 235 fission rate per atom	Rel 238 Capture rate	RCR*	238/235 fission ratio
		Coincid.	Coincid.	Height corrected
0	.4371 ± .34%	1.144 ± .45%	2.617 ± 0.6%	.0633 ± 1.3%
1.803	.4558 ± .33%	1.144 ± .45%	2.510 ± 0.6%	.0629 ± 1.3%
3.708	.5838 ± .35%	1.296 ± .44%	2.200 ± 0.6%	.0474 ± 2.0%
5.525	.9349 ± .24%	1.694 ± .4%	1.812 ± 0.6%	.0487 ± 0.8%

Run No.: D6

Date irradiation: 13/11/62

Time of start of irradiation: 0917 hours

Length of irradiation: 2 hours

Location of thermal foil: DIMPLE reflector (SEARCH TUBE C.15) U^{238} Cd Ratio = 27.9

Height correction depleted foil: -0.21%

Radius from cell centre (cm)	Rel 235 fission rate per atom	Rel 238 Capture rate	RCR*	238/235 fission ratio
		Coincid.	Coincid.	Height corrected
0	.4077 ± .5%	1.074 ± .7%	2.634 ± .8%	.0618 ± 1.2%
1.803	.4376 ± .7%	1.092 ± .5%	2.495 ± .8%	
3.708	.5566 ± .19%	1.226 ± .5%	2.203 ± .6%	.0470 ± 1.0%
5.525	.8747 ± .22%	1.578 ± .6%	1.804 ± .6%	.0479 ± 1.3%

Table 1 (Contd.)

Run No.: D7

Date irradiation: 15/11/62

Time of start of irradiation: 0831 hours

Length of irradiation: 2 hours

Location of thermal foil: DIMPLE reflector (SEARCH TUBE C.15) U^{238} Cd Ratio = 27.9

Height correction depleted foil: -0.21%

Radius from cell centre (cm)	Rel 235 fission rate per atom	Rel 238 Capture rate	RCR*	$^{238}/_{235}$ fission ratio
		Coincid.	Coincid.	Height corrected
0	.4089 ± .33	1.071 ± .54%	2.619 ± .65%	.0622 ±
1.803	.4292 ± .31%	1.098 ± .56%	2.558 ± ½65%	.0618 ± 1.5%
3.708	.5602 ± .20%	1.230 ± .54%	2.196 ± .6%	.0466 ± 0.8%
5.525	.8895 ± .32%	1.586 ± .7%	1.783 ± .7%	.0465 ± 2.2%

<u>Table 2</u>

<u>Summary of RCR* and fission ratio results</u>

(a) Relative modified conversion ratio (RCR*) measured by coincidence counting method

Cluster	Radius from cell centre (cm)	D5	D6	D7	Mean	Foil holder calibration factor	Corrected mean	Estimated Error %	Means corrected for non-thermal spectrum
J10	0	2.617	2.634	2.619	2.621	1.001	2.624	0.6	2.721
"	1.803	2.510	2.495	2.558	2.522	1.002	2.527	0.6	2.621
"	3.708	2.220	2.203	2.196	2.206	1.006	2.219	0.6	2.301
"	5.525	1.812	1.804	1.783	1.800	0.997	1.795	0.6	1.862

Radius (cm)	Relative error %	Total error %	Means corrected for smaller foil O.D.
0	0.8	+0.8 −3.1	2.694
1.803	0.8	+0.8 −3.1	2.595
3.708	0.8	+0.8 −3.1	2.278
5.525	0.8	+0.8 −3.1	1.856

(b) 238/235 fission ratio per atom

Cluster	Radius from cell centre (cm)	D5	D6	D7	Mean	Estimated error	Relative error %	Total Error %
J10	0	.0633	.0618	.0622	.0624	1.1%	1.2	10.0
"	1.803	.0629		.0618	.0624	1.3%	1.4	10.0
"	3.708	.0474	.0470	.0466	.0470	1.1%	1.2	10.0
"	5.525	.0487	.0479	.0465	.0477	1.1%	1.2	10.0

Table 3

Summary of U^{238} capture, U^{235} fission and U^{238} fission distributions (All in J10)

C_{xy} = mean ratio of run y to run x

(a) U^{238} Captive distribution (U^8)

Radius from cell centre (cm)	$U^8_1\ C_{11}$	$U^8_2\ C_{21}$	$U^8_3\ C_{31}$	Mean	Macros. Corr.	Corr. Mean	Stand. Dev. (from range)
0	1.144	1.139	1.133	1.139	0.98464	1.122	.004
1.803	1.144	1.158	1.162	1.155	0.98778	1.141	.006
3.708	1.296	1.301	1.301	1.299	0.99063	1.287	.002
5.525	1.694	1.674	1.678	1.682	0.99299	1.670	.007

(b) U^{235} Fission distribution (F^5)

Radius from cell centre (cm)	$F^5_1\ C_{11}$	$F^5_2\ C_{21}$	$F^5_3\ C_{31}$	Mean	Macros. Corr.	Corr. Mean	Stand. Dev. (from range)
0	0.4371	0.4313	0.4318	0.4334	0.98464	0.4267	.0018
1.803	0.4558	0.4629	0.4532	0.4573	0.98778	0.4517	.0033
3.708	0.5838	0.5888	0.5916	0.5881	0.99063	0.5826	.0026
5.525	0.9349	0.9253	0.9393	0.9332	0.99299	0.9266	.0048

(c) U^{238} Fission distribution (F^8)

Radius from cell centre (cm)	$F_1^8\ C_{11}$	$F_2^8\ C_{21}$	$F_3^8\ C_{31}$	Mean	Macros. Corr	Corr. Mean	Stand. Dev.
0	.0277	.0272	.0275	.0275	0.98464	.0271	.0002
1.803	.0287		.0287	.0287	0.98778	.0283	.0002
3.708	.0277	.0283	.0283	.0281	0.99063	.0278	.0002
5.525	.0455	.0453	.0448	.0452	0.99299	.0449	.0003

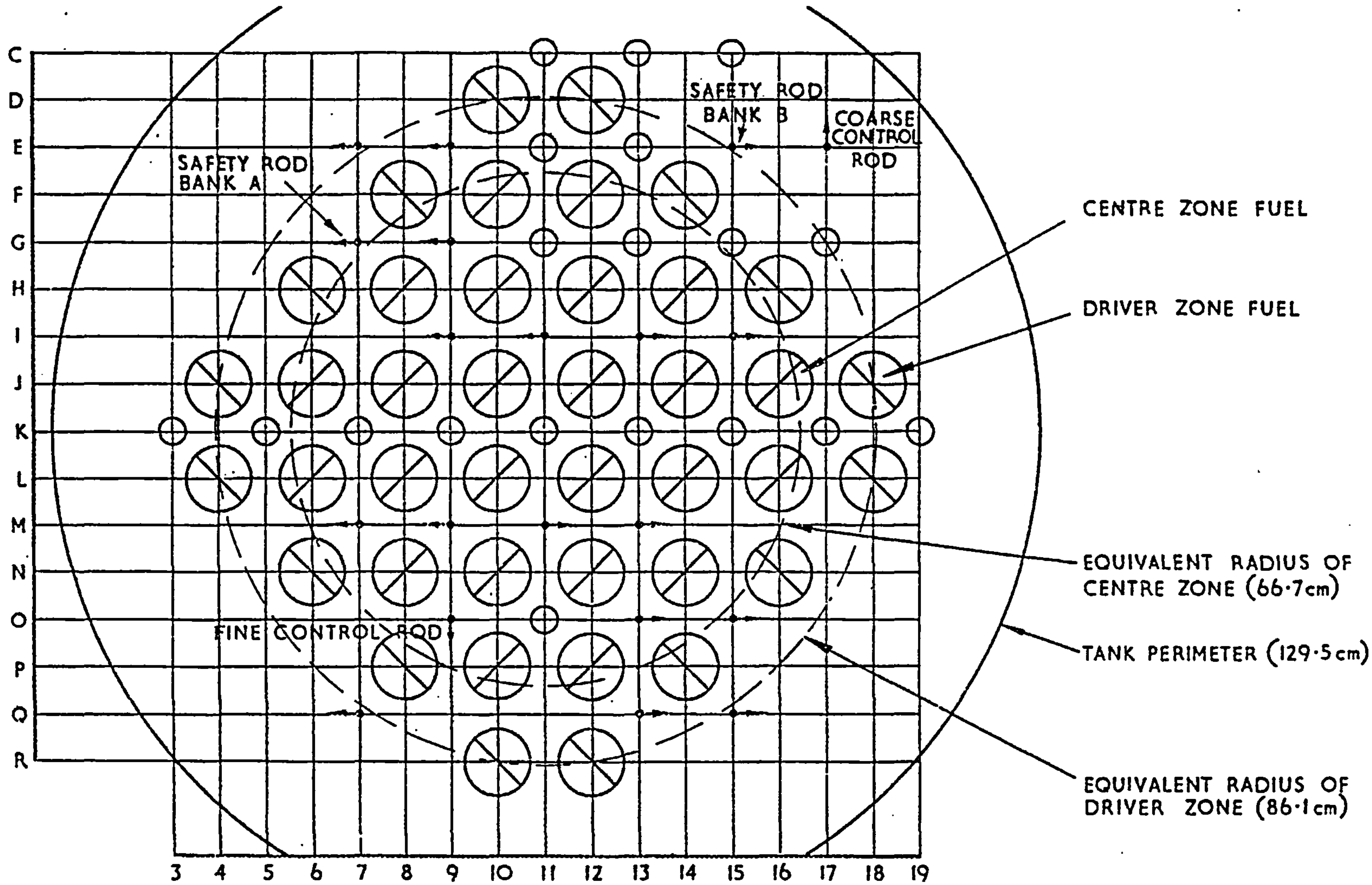

FIG.1 PLAN VIEW OF TANK TOP

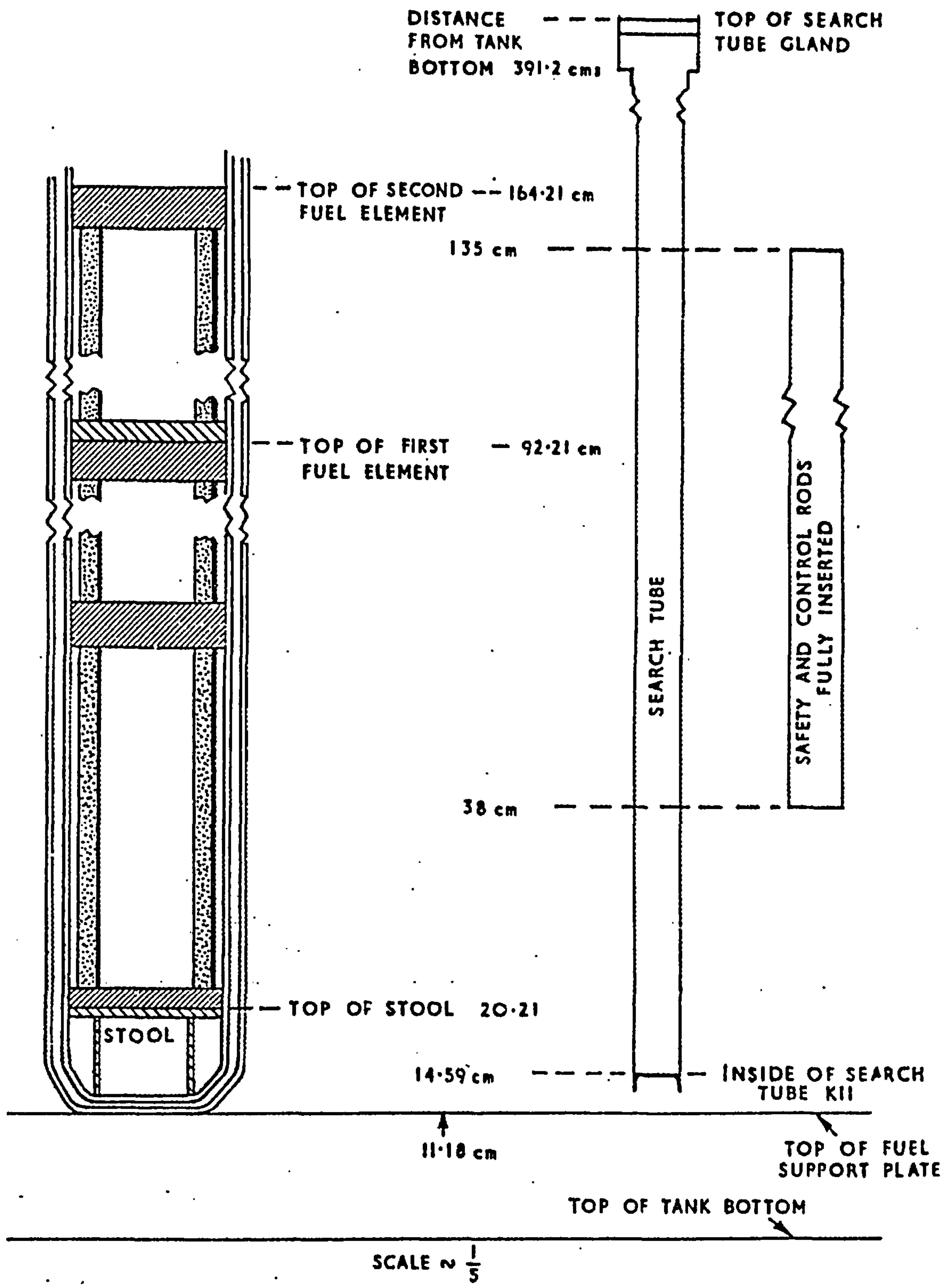

FIG.2 DETAILS OF INNER ZONE FUEL, SEARCH TUBES, AND SAFETY RODS

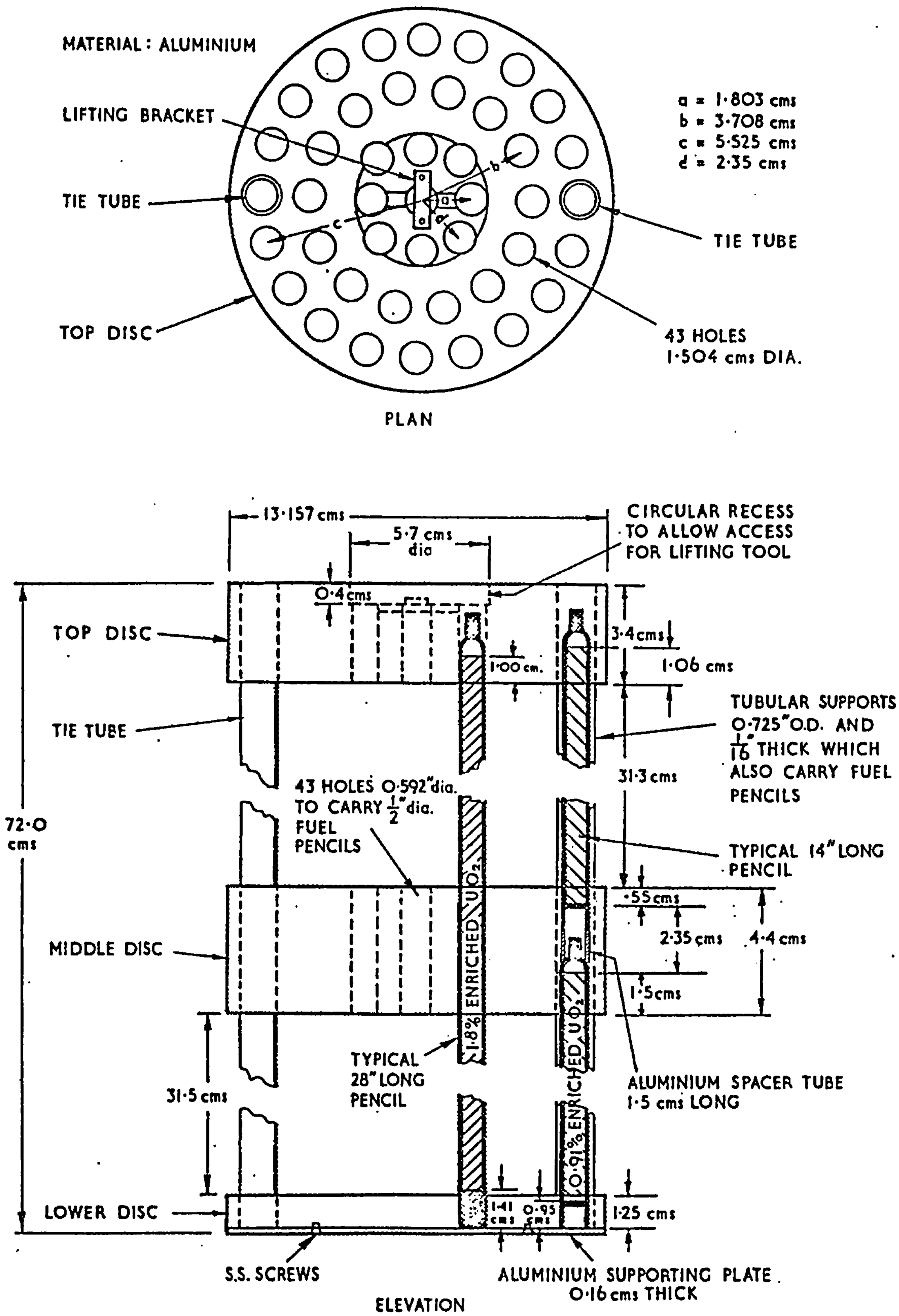

FIG.3 DETAILS OF INNER ZONE FUEL CLUSTER

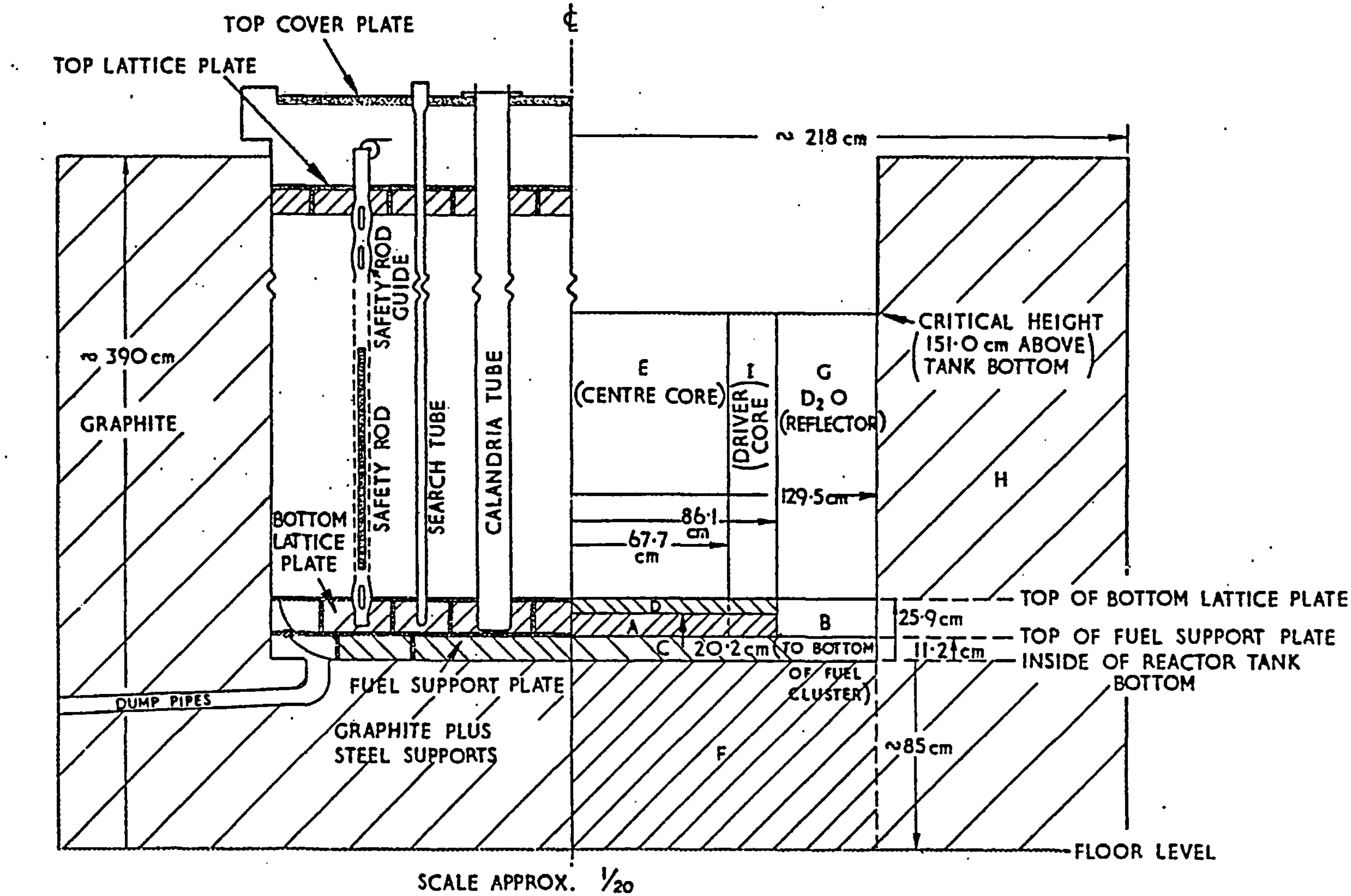

FIG. 4(a) SECTION THROUGH REACTOR

FIG 4(b) SIMPLIFIED SECTION THROUGH REACTOR GIVING REGIONS OF DIFFERENT PHYSICAL PROPERTIES

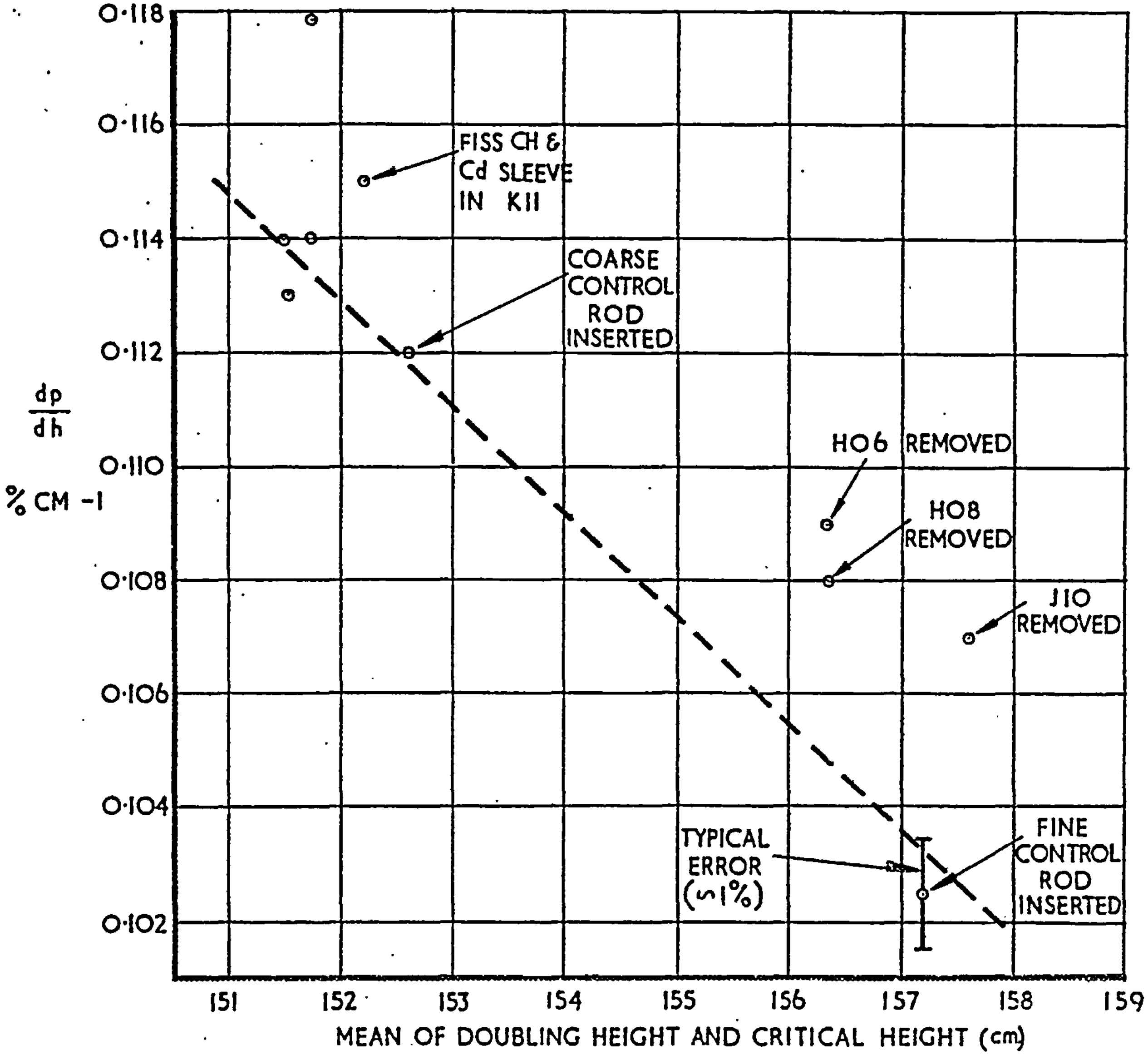

NOTE
DOTTED LINE IS THROUGH VALUES $d\rho/dh$ MEASURED WITH CONTROL ROD INSERTIONS ONLY (SEE SECTION 4)

FIG.5 $d\rho/dh$ VS MEAN HEIGHT OF MEASUREMENT

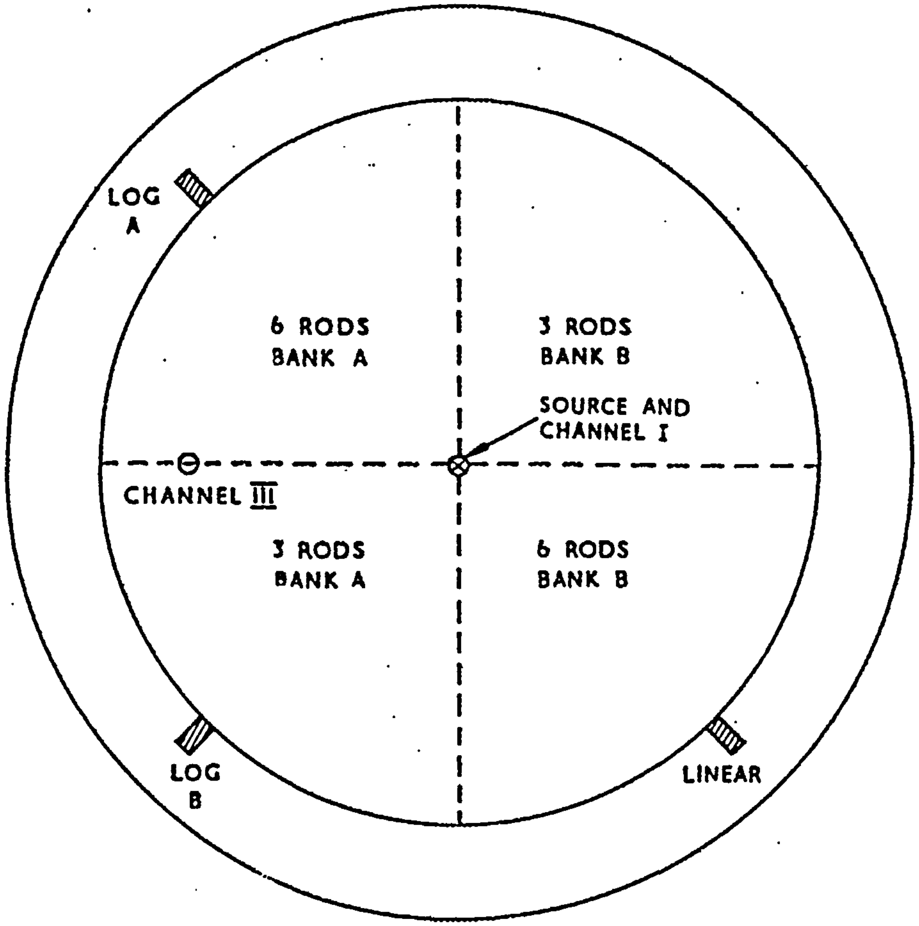

AXIAL POSITIONS:-

SOURCE ~ 16 cm FROM TANK BOTTOM

CHANNEL I ~ 170 cm FROM TANK BOTTOM

INSTALLED CHAMBERS AND CHANNEL III

~80 cm. FROM TANK BOTTOM

FIG.6 SOURCE AND DETECTOR POSITIONS FOR SUB-CRITICAL REACTIVITY MEASUREMENTS

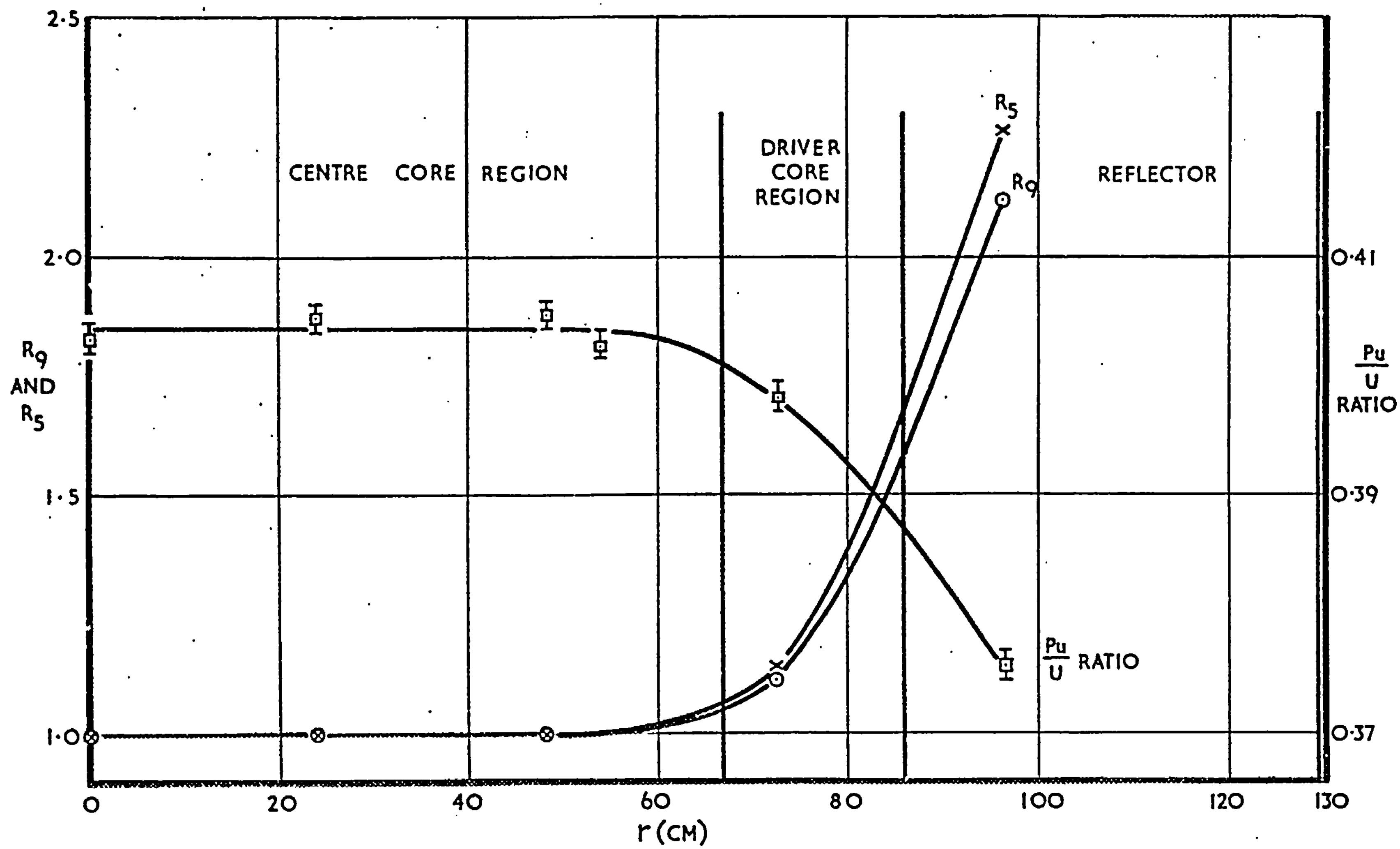

FIG. 7 PLUTONIUM TO URANIUM RATIO AND PLUTONIUM AND URANIUM RELATIVE CADMIUM RATIOS AS FUNCTIONS OF RADIUS

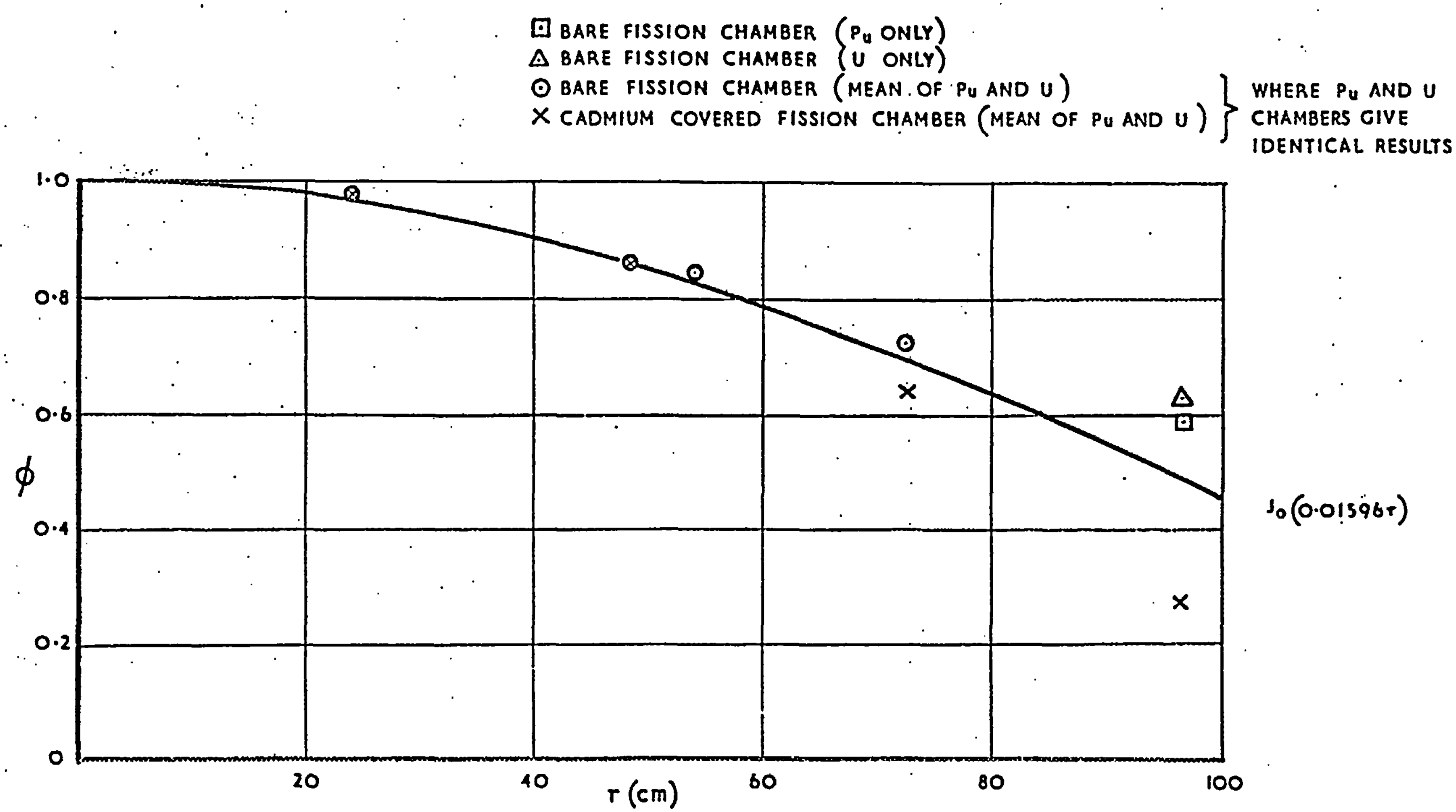

FIG.8 RADIAL REACTION RATES (NORMALISED TO
TO UNITY AT CORE CENTRE)

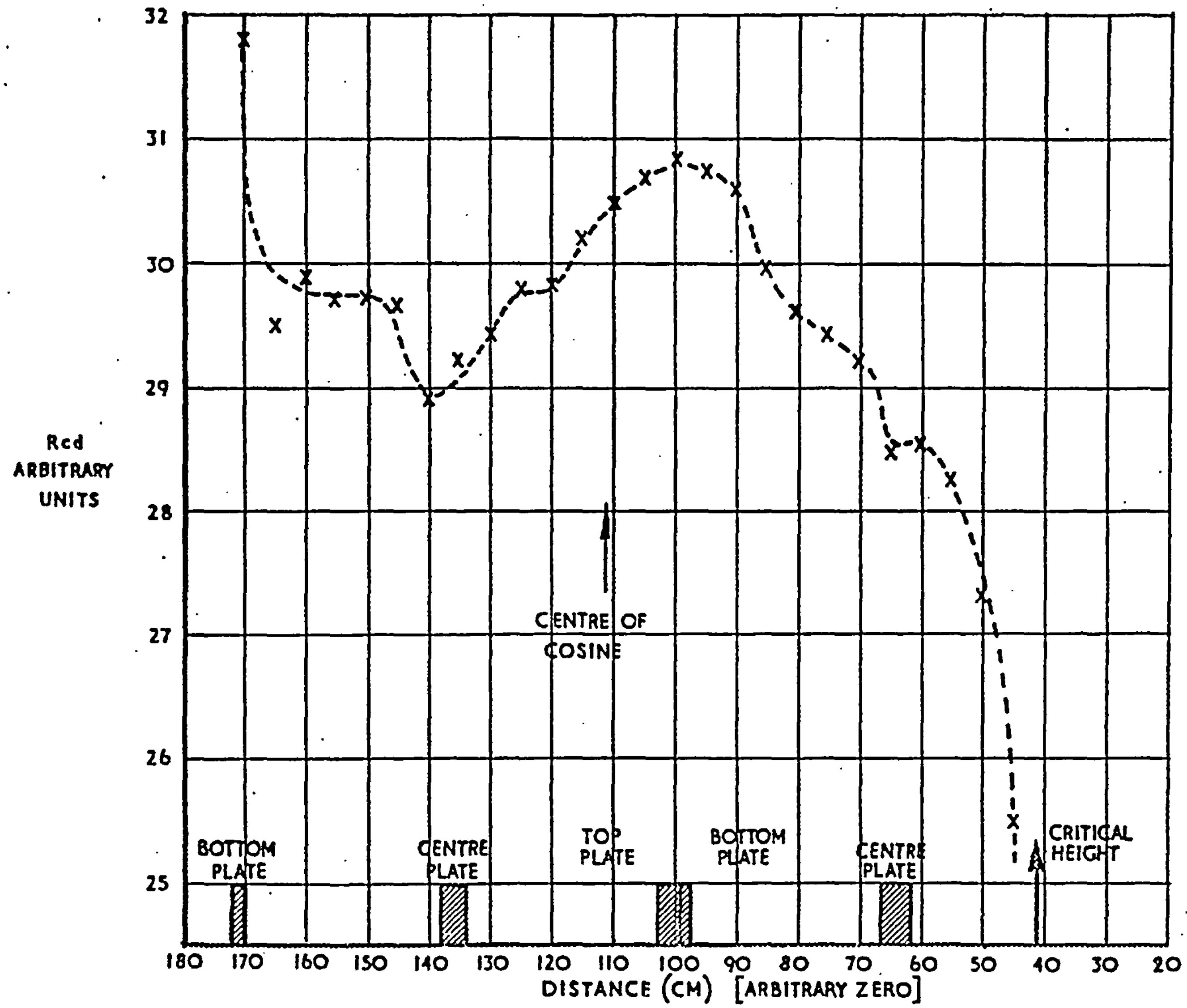

FIG.9 AXIAL CADMIUM RATIO DISTRIBUTION IN KII

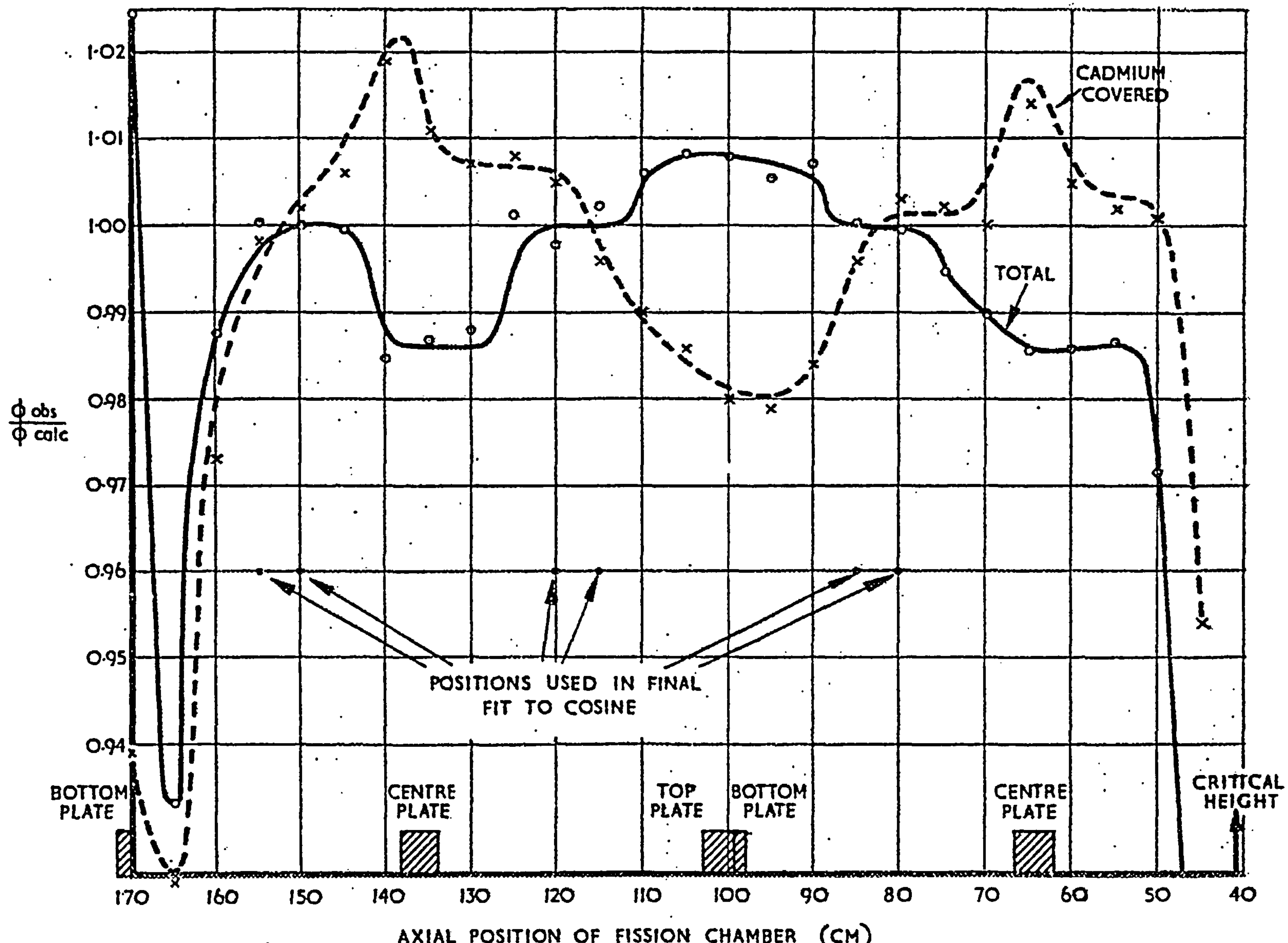

FIG.10 ϕ_{obs}/ϕ_{calc} IN SEARCH TUBE KII (U235 FISSION CHAMBER)

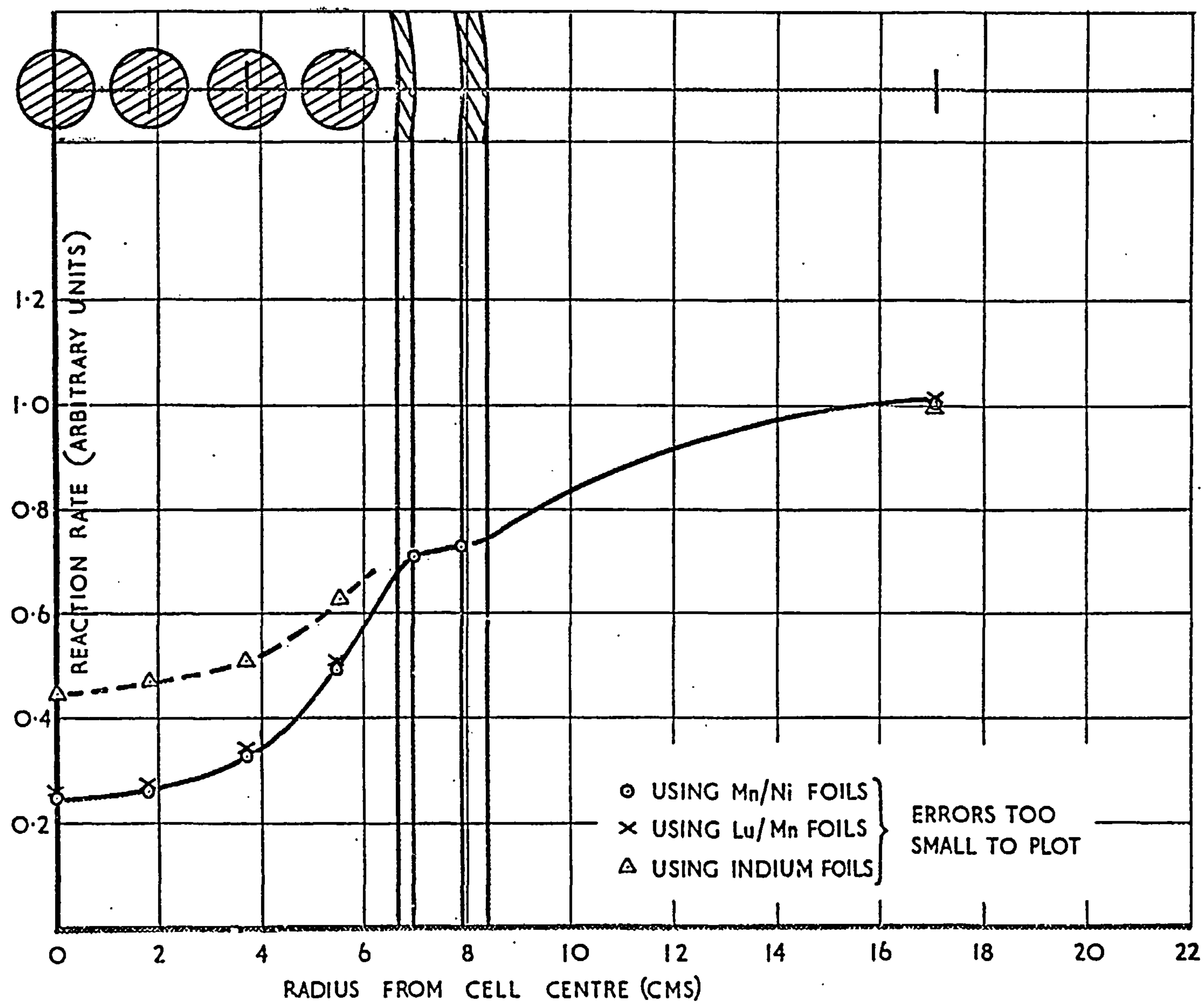

FIG. 11 MANGANESE AND INDIUM REACTION RATE RATIOS IN THE LATTICE CELL

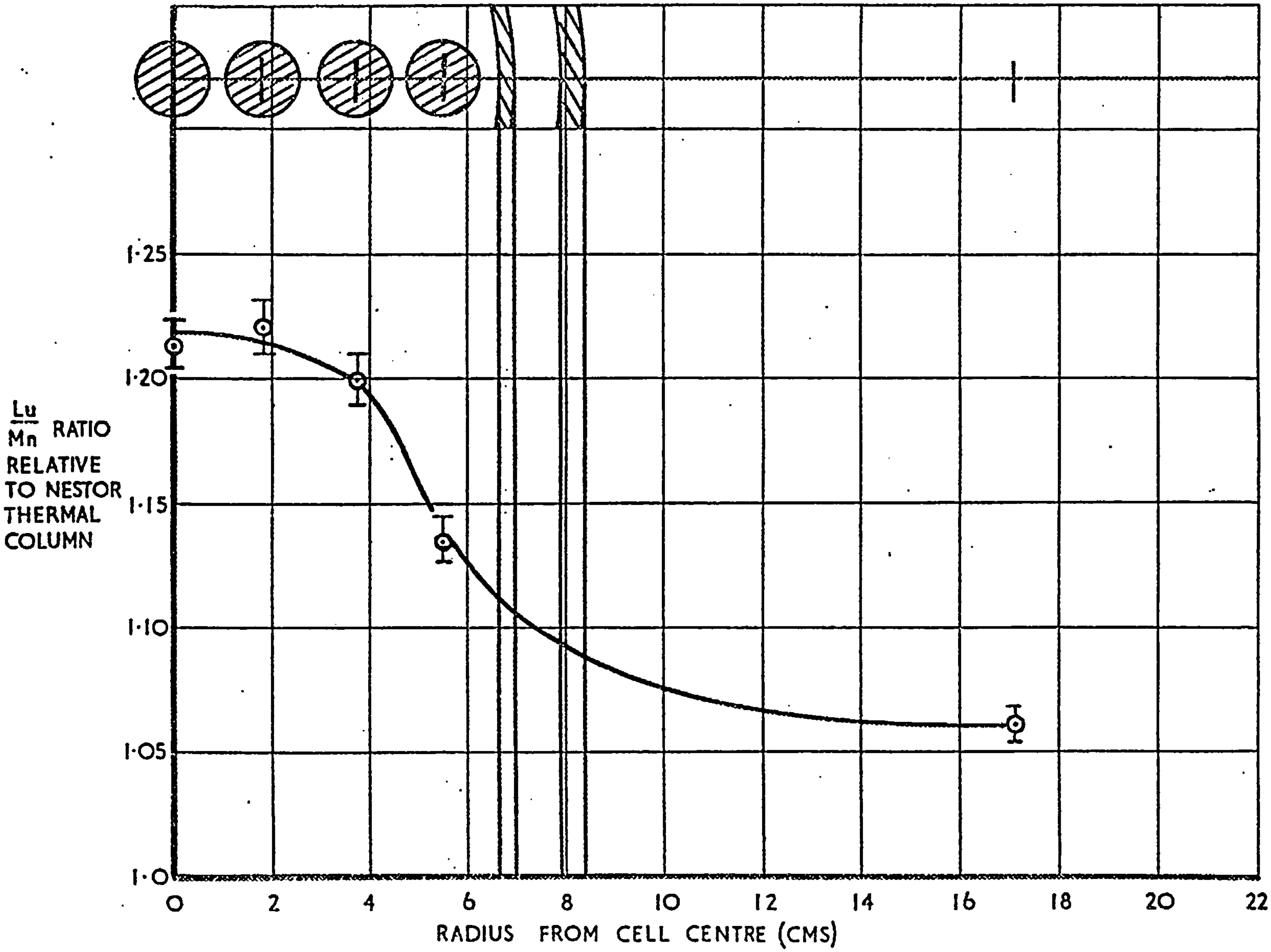

FIG. 12 LUTECIUM TO MANGANESE RATIO IN THE LATTICE CELL

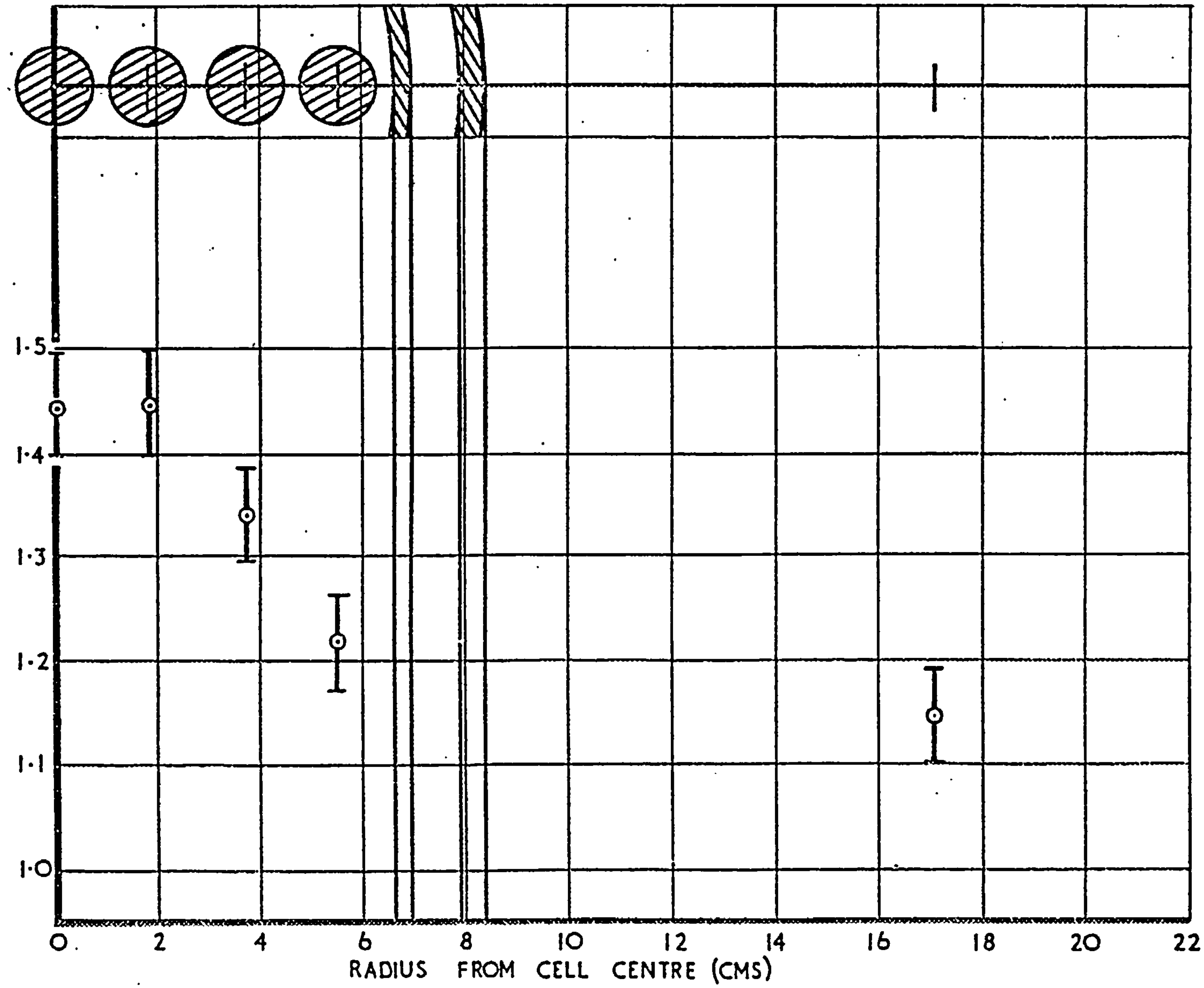

FIG. 13 PLUTONIUM TO URANIUM RATIO IN THE LATTICE CELL

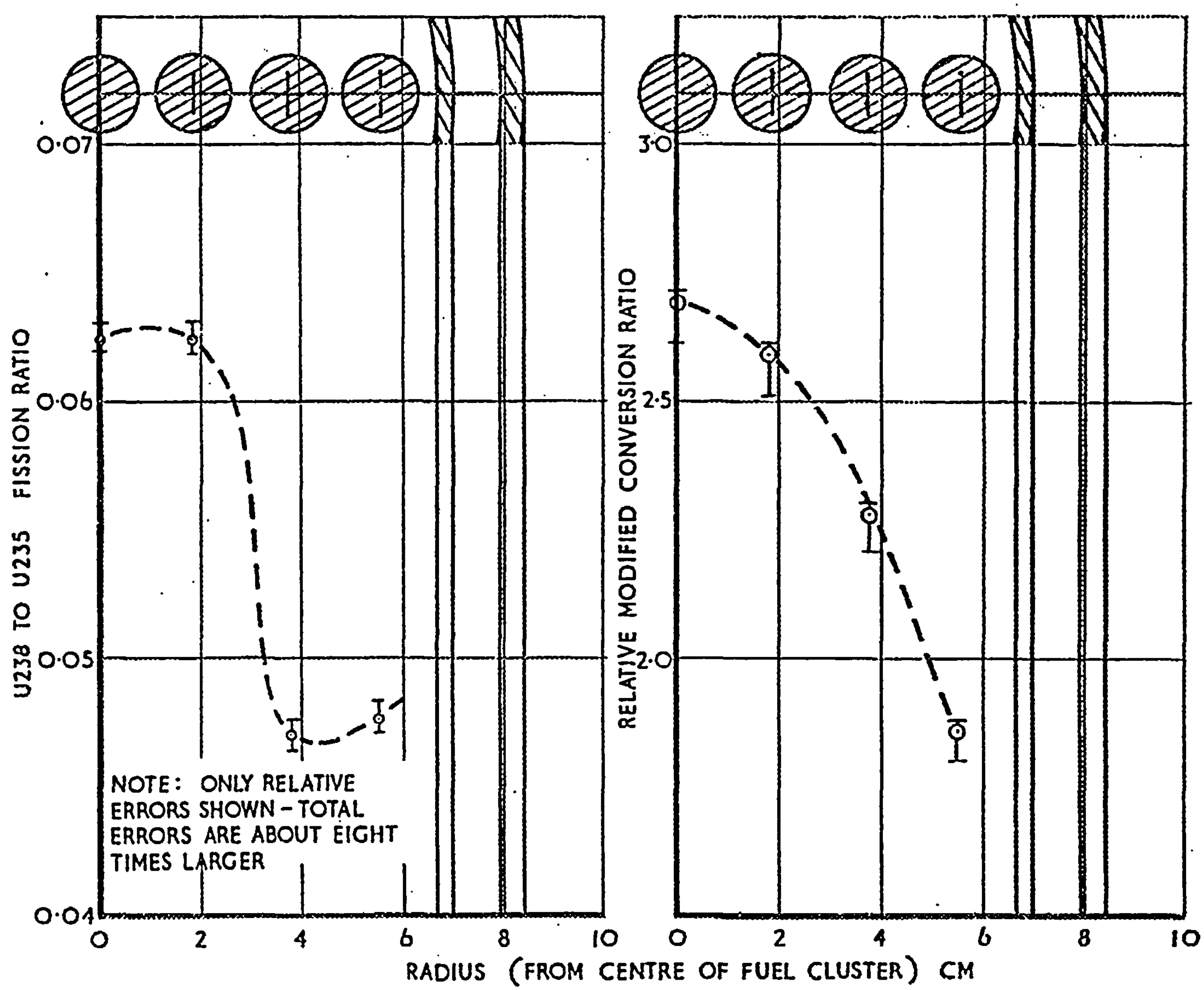

FIG.14 (a) U238/U238 FISSION RATIO IN THE FUEL

FIG.14 (b) RELATIVE CONVERSION RATIO IN THE FUEL

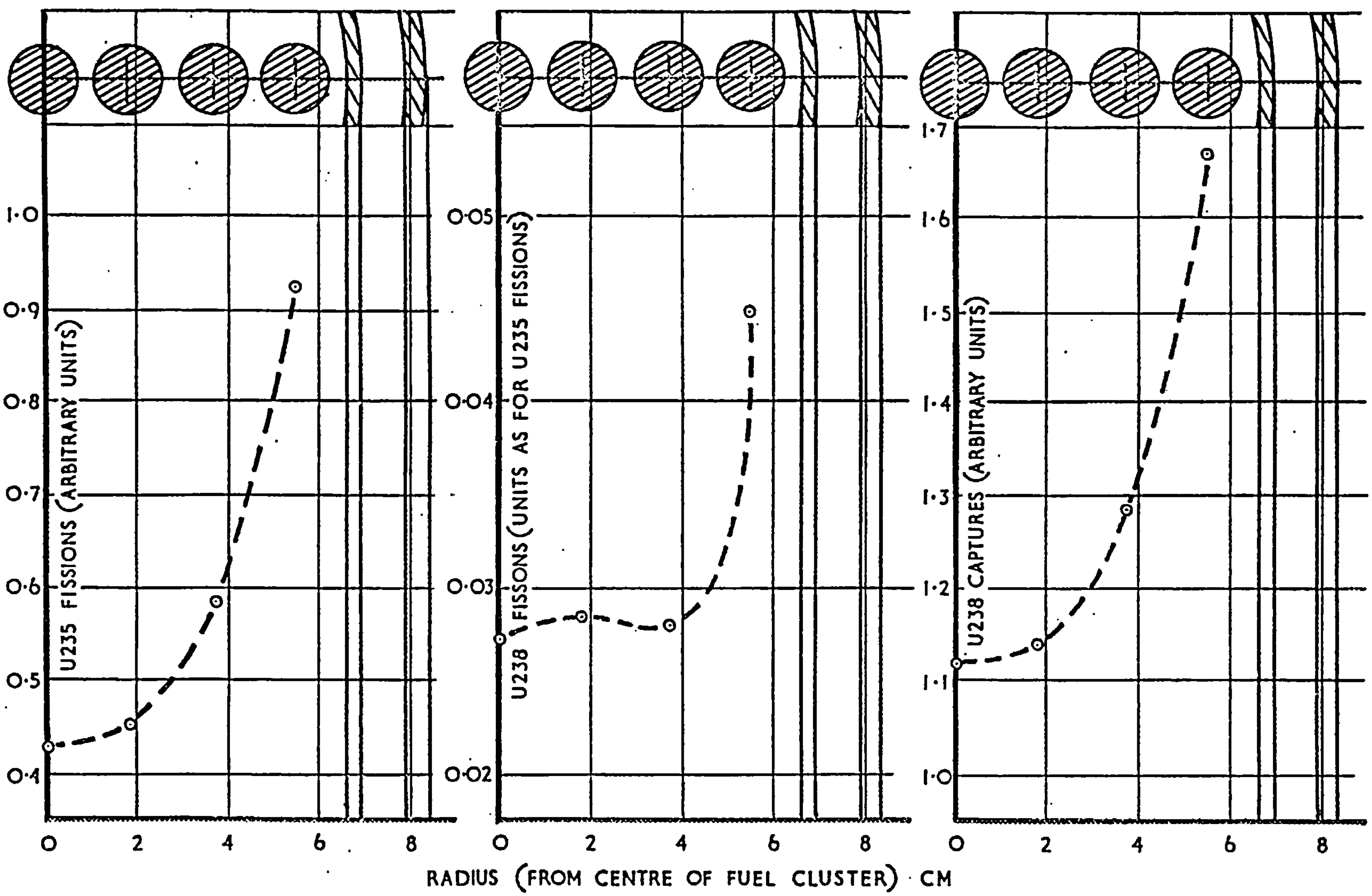

FIG. 15 U235 FISSION, U238 FISSION, AND U238 CAPTURE IN THE FUEL (RANDOM ERRORS TOO SMALL TO PLOT)